Mycobacterium tuberculosis-specific CD4$^+$ and CD8$^+$ T cells differ in their capacity to recognize infected macrophages

Jason Yang[1], Daniel Mott[1], Rujapak Sutiwisesak[1], Yu Jung Lu[1], Fiona Raso[1], Britni Stowell[1], Greg Babunovic[2], Jinhee Lee[1], Steve Carpenter[1], Sing Sing Way[3], Sarah Fortune[2], Sam Behar[1]

1. Department of Microbiology and Physiological Systems, University of Massachusetts Medical School, Worcester, Massachusetts, USA.
2. Department of Immunology and Infectious Diseases, Harvard T.H. Chan School of Public Health, Boston, Massachusetts, USA.
3. Division of Infectious Disease, Cincinnati Children's Hospital, Cincinnati, Ohio, USA

Correspondence:

Samuel M. Behar

E-mail address: samuel.behar@umassmed.edu (SMB)

Abstract

Containment of *Mycobacterium tuberculosis* (Mtb) infection requires T cell recognition of infected macrophages. Mtb has evolved to tolerate, evade, and subvert host immunity. Despite a vigorous and sustained $CD8^+$ T cell response during Mtb infection, $CD8^+$ T cells make limited contribution to protection. Here, we ask whether the ability of Mtb-specific T cells to restrict Mtb growth is related to their capacity to recognize Mtb-infected macrophages.

We derived $CD8^+$ T cell lines that recognized the Mtb immunodominant epitope $TB10.4_{4-11}$ and compared them to $CD4^+$ T cell lines that recognized $Ag85b_{240-254}$ or $ESAT6_{3-17}$. While the $CD4^+$ T cells recognized Mtb-infected macrophages and inhibited Mtb growth in vitro, the TB10.4-specific $CD8^+$ T cells neither recognized Mtb-infected macrophages nor restricted Mtb growth. TB10.4-specific $CD8^+$ T cells recognized macrophages infected with *Listeria monocytogenes* expressing TB10.4. However, over-expression of TB10.4 in Mtb did not confer recognition by TB10.4-specific $CD8^+$ T cells. Importantly, $CD8^+$ T cells recognized macrophages pulsed with irradiated Mtb, indicating that macrophages can efficiently cross-present the TB10.4 protein and raising the possibility that viable bacilli might suppress cross-presentation. Importantly, polyclonal $CD8^+$ T cells specific for Mtb antigens other than TB10.4 recognized Mtb-infected macrophages in a MHC-restricted manner.

As TB10.4 elicits a dominant $CD8^+$ T cell response that poorly recognizes Mtb-infected macrophages, we propose that TB10.4 acts as a decoy antigen. Moreover, it appears that this response overshadows subdominant $CD8^+$ T cell response that can recognize Mtb-infected macrophages. The ability of Mtb to subvert the $CD8^+$ T cell response may explain why $CD8^+$ T cells make a disproportionately small contribution to host defense compared to $CD4^+$ T cells. The selection of Mtb antigens for vaccines has focused on antigens that generate immunodominant responses. We propose that establishing whether vaccine-elicited, Mtb-specific T cells recognize Mtb-infected macrophages could be a useful criterion for preclinical vaccine development.

44 ## Introduction

45 Unlike most disease-causing pathogens, *Mycobacterium tuberculosis* (Mtb), the cause of
46 tuberculosis (TB), persists in humans because of its highly evolved ability to evade and subvert
47 the host immunity [1]. Mtb subverts vesicular trafficking, prevents phagolysosome fusion, and
48 replicates in an intracellular niche within macrophages, allowing it to evade detection by humoral
49 immunity [2]. Mtb also delays the initiation and recruitment of T cell immunity to the lung,
50 promoting the establishment of a persistent infection [3]. Despite these challenges, T cell
51 immunity does occur and plays an essential role in controlling the infection in both mice and
52 humans [3-5]. With 10 million new TB cases annually, an effective vaccine would offer a cost-
53 effective way to prevent TB and attenuate this persistent global pandemic. Given the importance
54 of T cells during host defense, strategies for TB vaccines largely aim at generating memory T
55 cells rather than neutralizing antibodies. Most subunit vaccines incorporate immunodominant Mtb
56 antigens, which elicit large T cell responses [6]. Several immunodominant antigens have been
57 identified in the murine TB model, including Ag85a, Ag85b, CFP-10, ESAT-6 and TB10.4 [7]. T
58 cell responses to these antigens are also frequently detectable in Mtb-infected people, and these
59 highly prevalent responses represent the basis for TB immunodiagnostic tests [8]. By
60 incorporating these immunodominant antigens into vaccines, the expectation is that antigen-
61 specific T cells will contain the infection before Mtb can establish a niche and evade host immunity
62 [6].

63 T cell recognition of Mtb-infected macrophages is fundamental to containment of TB
64 infection. Srivastava et al elegantly showed this by using mixed bone marrow (BM) chimeric mice
65 made from wild type (WT) and major histocompatibility complex class II (MHC class II) deficient
66 BM [9]. Following infection, polyclonal $CD4^+$ T cells suppressed Mtb growth more efficiently in
67 MHC class II-expressing cells than in MHC class II-deficient cells. This data convincingly argues
68 that cognate recognition (i.e., T cell receptor (TCR) mediated recognition) of infected cells by

69 polyclonal $CD4^+$ T cells limits bacterial growth. However, whether this protection comes from T
70 cells recognizing immunodominant or subdominant antigens remains unknown. In fact, even
71 though many presume that Mtb-infected cells present immunodominant antigens, the data
72 validating this assumption is surprisingly inconsistent. While there is consensus that Mtb-infected
73 cells present ESAT-6, the data concerning Ag85b presentation is more complicated [10-13].
74 $Ag85b_{241-256}$ elicits a $CD4^+$ T cell response early after infection, but Mtb reduces Ag85b
75 production within three weeks after in vivo infection [12]. Thus, while $Ag85b_{241-256}$-specific $CD4^+$
76 T cells can recognize dendritic cells (DC) from infected mice 14 days post infection [14], there is
77 little recognition of Mtb-infected cells by $Ag85b_{241-256}$-specific $CD4^+$ T cells in vivo by day 21 [12].
78 Furthermore, Mtb has other mechanisms to evade T cell recognition, including dysregulating MHC
79 class II expression and inhibiting antigen presentation by stimulating antigen export by the
80 infected antigen presenting cells (APCs) [1, 12, 13, 15]. Whether the immunodominant antigens
81 recognized by $CD8^+$ T cells are presented by Mtb-infected macrophages remains unknown. Here,
82 we investigated cognate T cell recognition of Mtb-infected macrophages by $CD8^+$ T cells specific
83 to the immunodominant antigen TB10.4.

84 TB10.4 (EsxH) is an ESAT-6-like protein secreted by the ESX-3 type VII secretion system,
85 important in iron and zinc acquisition, and essential for Mtb growth in vitro and in vivo [16, 17].
86 Following Mtb infection, TB10.4 is a target of $CD4^+$ and $CD8^+$ T cell responses in humans and
87 mice [18-22]. In Mtb-infected mice, TB10.4 elicits immunodominant responses in both BALB/c
88 and C57BL/6 mice, and 30-50% of lung $CD8^+$ T cells are specific to single epitopes (S1 Fig) [18,
89 19]. Whether these TB10.4-specific $CD8^+$ T cells can mediate protection is unclear. Adoptive
90 transfer of TB10.4-specific $CD8^+$ T cells into Mtb-infected, immunocompromised mice reduces
91 the bacterial burden and promotes host survival [19]. However, despite eliciting large numbers of
92 TB10.4-specific $CD8^+$ T cells, a vaccine incorporating the H-2 K^b-restricted epitope, $TB10.4_{4-11}$,
93 fails to protect mice from Mtb infection [23]. We hypothesize that the inability of TB10.4-specific

94 $CD8^+$ T cells to mediate protection is due to inefficient recognition of Mtb-infected macrophages.

95 We used primary $CD4^+$ and $CD8^+$ T cells lines to investigate the recognition of Mtb-infected
96 macrophages by T cells specific to Ag85b, ESAT-6, or TB10.4. Ag85b- and ESAT-6-specific $CD4^+$
97 T cells recognized Mtb-infected macrophages, but under the same conditions, TB10-specific
98 $CD8^+$ T cells did not recognize infected macrophages or inhibit bacterial growth. This was true
99 even upon examination of numerous conditions and permutations including length of infection,
100 duration of T cell and macrophage co-culture, and multiplicity of infection. TB10.4-specific $CD8^+$
101 T cells did recognize macrophages infected with recombinant *Listeria monocytogenes* expressing
102 TB10.4, but only if the bacilli could escape into the cytosol. However, overexpressing TB10.4 in
103 Mtb did not confer recognition. Importantly, macrophages pulsed with irradiated bacteria efficiently
104 cross-presented TB10.4 to $CD8^+$ T cells, suggesting that live Mtb actively inhibited presentation.
105 Interestingly, polyclonal $CD8^+$ T cells specific for Mtb antigens other than TB10.4 recognized Mtb-
106 infected macrophages in a MHC class I-restricted manner. Thus, while TB10.4-specific $CD8^+$ T
107 cells do not recognize Mtb-infected macrophages, there exist other $CD8^+$ T cells that recognize
108 subdominant antigens presented by Mtb-infected cells. Based on these data, we propose that
109 TB10.4 is a decoy antigen: it elicits a massive and persistent $CD8^+$ T cell response, which cannot
110 recognize Mtb-infected macrophages. Such a decoy antigen may distract the $CD8^+$ response from
111 focusing on subdominant antigens presented by infected cells, leading to evasion from host
112 immunity.
113

114 ## Results

115 **TB10.4-specific CD8$^+$ and Ag85b-specific CD4$^+$ T cell lines sensitively recognize**
116 **their cognate antigens.**

117 To study T cell recognition of Mtb-infected macrophages, we established antigen-specific
118 T cell lines, which unlike T cell hybridomas, facilitate the study of T cell function as well as
119 recognition. The TB10.4$_{4-11}$-specific CD8$^+$ T cell line, referred hereafter as TB10Rg3, has a distinct
120 TCR cloned originally from TB10.4$_{4-11}$-tetramer$^+$ CD8$^+$ T cells isolated from infected mice and
121 expressed in retrogenic mice [19]. The Ag85b$_{240-254}$-specific CD4$^+$ T cell line, referred hereafter as
122 P25 cells, was derived from P25 TCR transgenic mice [24]. To confirm their antigen-specificity,
123 we co-cultured the P25 or TB10Rg3 T cells with thioglycolate-elicited peritoneal macrophages
124 (TGPMs) pulsed with or without their cognate peptides and then measured their expression of
125 CD69 and Nur77. While both CD69 and Nur77 are T cell activation markers, increases in Nur77
126 expression indicate TCR-mediated activation more specifically [25, 26]. After co-culture with
127 TGPMs pulsed with Ag85b$_{241-256}$ peptide, Nur77 expression by P25 cells peaked after 2 hours
128 (Fig 1a, b), while CD69 expression continued to increase (Fig 1c, d). TB10Rg3 T cells exhibited
129 similar Nur77 and CD69 expression patterns after their co-culture with TGPMs pulsed with the
130 TB10.4$_{4-11}$ peptide (IMYNYPAM) but not with a control peptide (IMANAPAM) (Fig 1e-h). Since the
131 increase in Nur77 expression was transient, we next tested whether CD69 and IFNγ could be
132 useful markers of antigen recognition for longer experiments. During 72 hours of co-culture with
133 peptide-pulsed TGPMs, P25 and TB10Rg3 T cells continued to express CD69 and secreted IFNγ
134 in a peptide dose-dependent manner (Fig 1i-l). These experiments show that P25 and TB10Rg3
135 T cells can recognize their cognate antigens presented by TGPMs, both in short-term and long-
136 term co-culture assays.

137

138

139 **Ag85b-specific CD4$^+$ T cells, but not TB10.4-specific CD8$^+$ T cells, restrict**
140 **intracellular bacterial replication.**

141 Given that a primary function of T cells during Mtb infection is to restrict bacterial growth,
142 we determined whether these T cell lines could limit intracellular mycobacterial growth *in vitro*.
143 We infected TGPMs with H37Rv, a virulent Mtb strain that expresses both TB10.4 and Ag85b in
144 vitro [21, 27]. To assess whether any bacterial growth inhibition observed was dependent on
145 cognate recognition, we infected both MHC-matched (i.e., H-2^b) and mismatched (i.e., H-2^k)
146 macrophages. T cells were added on day 1 post-infection, and the number of colony forming units
147 (CFU) was assayed 96 hours later. In the absence of T cells, Mtb grew significantly ($p<0.01$) (Fig
148 2). P25 T cells significantly inhibited intracellular bacterial growth in H37Rv-infected TGPMs
149 ($p<0.0001$). Addition of Ag85b peptide to the infected macrophages did not further enhance the
150 ability of P25 T cells to inhibit bacterial growth, suggesting that their activation was maximal. As
151 expected, P25 T cells only inhibited bacterial growth in MHC-matched macrophages, indicating
152 that growth inhibition mediated by T cells required cognate recognition under these conditions.

153 In contrast, TB10Rg3 T cells did not inhibit bacterial growth (Fig 2). We considered
154 whether the inability of TB10Rg3 to inhibit bacterial growth was due to a lack of recognition of the
155 infected macrophages or a defect in the T cells' effector functions. When Mtb-infected TGPMs
156 were pulsed with the TB10.4$_{4-11}$ peptide for one hour prior to adding the T cells, TB10Rg3 T cells
157 significantly reduced bacterial growth ($p<0.0001$) (Fig 2a). Thus, under the same conditions where
158 P25 T cells significantly suppressed intracellular Mtb growth in a MHC-restricted manner,
159 TB10Rg3 T cells failed to inhibit bacterial growth.

160 We next considered whether the inability of TB10Rg3 to restrict intracellular bacterial
161 growth was true for other TB10.4$_{4-11}$-specific CD8$^+$ T cells. To obtain TCRs representative of other
162 clonally expanded TB10.4$_{4-11}$-specific CD8$^+$ T cells, TB10.4$_{4-11}$-tetramer$^+$ CD8$^+$ T cells from Mtb-
163 infected C57BL/6 mice were single cell sorted, and both the TCR CDR3α and CDR3β regions

164 were sequenced (Fig S2). Three TCRs representative of clonally expanded T cells (TB10RgL,
165 TB10RgR, and TB10RgQ) were cloned (Fig S2). In addition, a fourth TCR (TB10RgP), not
166 previously identified by NexGen sequencing, was also cloned. All these TCRs responded
167 specifically to the TB10.4_{4-11} epitope and expressed TCRs distinct from TB10Rg3 (Fig S3). We
168 generated T cell lines from these retrogenic mice, as described for TB10Rg3. TB10RgP,
169 TB10RgL, and TB10RgR did not inhibit bacterial growth (Fig 2b). However, if the Mtb-infected
170 macrophages were pulsed with the TB10.4_{4-11} peptide before T cell addition, then TB10RgP,
171 TB10RgL, and TB10RgR T cells all inhibited bacterial growth significantly (Fig 2b). Since TB10.4_{4-}
172 $_{11}$-specific $CD8^+$ T cells only inhibited bacterial growth when their cognate peptide was added to
173 Mtb-infected macrophages, we conclude that, although they express the effector function required
174 to restrict intracellular bacterial growth, these TB10.4_{4-11}-specific $CD8^+$ T cells do not recognize
175 Mtb-infected macrophages.
176
177
178 **Ag85b-specific $CD4^+$ T cells, but not TB10.4-specific $CD8^+$ T cells, recognize Mtb-**
179 **infected macrophages.**
180 To further investigate TB10Rg3 and P25 T cells recognition of Mtb-infected cells, we next
181 investigated the kinetics of Mtb antigen presentation. After Mtb infection, TGPMs were cultured
182 for various lengths of time before adding the T cells. To assay antigen presentation, we added
183 the T cells for two hours and then measured Nur77 and CD69 (see Fig 1 for kinetics). When
184 added immediately after infection (i.e., day 0), P25 T cells recognized Mtb-infected macrophages
185 based on the induction of Nur77 and CD69 (Fig 3a, b). Under these conditions, there was no
186 increase in Nur77 or CD69 expression by TB10Rg3 T cells (Fig 3c, d). We next chose later time
187 points, which might allow Mtb to adapt to the intracellular environment and potentially let the
188 TB10.4 antigen accumulate. TB10Rg3 T cells were added to infected macrophages on days 1, 3,

189 or 5 post-infection. Again, we did not observe any increase in Nur77 or CD69 expression (Fig 3e,
190 f). As a control for T cell health and function, we co-cultured TB10.4$_{4-11}$-peptide-pulsed-,
191 uninfected-macrophages with the TB10Rg3 T cells and observed significant increases in their
192 Nur77 and CD69 expression (Fig 3).

193 Despite assessing recognition on multiple days, we considered whether the short assay
194 period (i.e. 2 hours) might not detect recognition of Mtb-infected macrophages by TB10Rg3 T
195 cells, especially if presentation of TB10.4 is inefficient or asynchronous. Therefore, we used IFNγ
196 production as a cumulative indicator of T cell activation during a 72-hour co-culture experiment.
197 Since cytokine-driven activation (e.g., IL-12, IL-18) can stimulate IFNγ production by T cells
198 independently of TCR signaling, we used MHC-matched (H-2^b) or mismatched (H-2^k) TGPM to
199 assess cognate recognition [26, 28-30]. As the infectious dose (MOI, multiplicity of infection)
200 increased, P25 T cells produced more IFNγ when co-cultured with MHC-matched, but not MHC-
201 mismatched, Mtb-infected TGPMs (Fig 3g). In contrast, TB10Rg3 T cells did not produce IFNγ
202 when co-cultured with Mtb-infected TGPMs (Fig 3h). As before, TB10Rg3 T cells produced IFNγ
203 when co-cultured with uninfected macrophages pulsed with the TB10.4$_{4-11}$ peptide (Fig 3h).

204 We next used the TB10.4$_{4-11}$-specific CD8$^+$ T cell lines TB10RgP, TB10RgL and TB10RgR
205 to address whether TB10.4$_{4-11}$-specific CD8$^+$ T cells other than TB10Rg3 can recognize Mtb-
206 infected macrophages. While the TB10RgP, TB10RgL, and TB10RgR CD8$^+$ T cell lines produced
207 IFNγ when cultured with uninfected macrophages pulsed with the TB10.4$_{4-11}$ peptide, none
208 produced IFNγ following a 72-hour co-culture with Mtb-infected macrophages (Fig 3i). These data
209 show that, regardless of the time point of T cell addition or the length of co-culture, P25 T cells,
210 but not TB10.4$_{4-11}$-specific CD8$^+$ T cells, recognized Mtb-infected macrophages, based on their
211 increased Nur77 and CD69 expression as well as their IFNγ production.

212

213 **TB10.4-specific CD8$^+$ T cells do not recognize lung cells from Mtb-infected mice.**

214 During *in vivo* infection, Mtb infects a variety of myeloid cells, and this diversity changes

215 over the course of the infection [31-33]. We considered that lung myeloid cells from Mtb-infected
216 mice are more physiologically relevant than TGPMs. Thus, we isolated MHC class II$^+$ lung cells
217 from Erdman-infected, RAG-1-deficient mice 4 weeks post-infection and tested their ability to
218 present Mtb antigens to TB10Rg3 T cells. We used RAG-1-deficient mice because of the
219 possibility that CD8$^+$ T cells in the lungs of Mtb-infected, wild type mice may recognize and
220 eliminate any lung cells presenting the TB10.4 antigen. Since Mtb downregulates Ag85b
221 expression by 3 weeks post infection [11, 12], we used an ESAT-6-specific CD4$^+$ T cell line
222 derived from C7 transgenic mice, which we refer to as C7 T cells [10, 34]. The immunodominant
223 antigen ESAT-6 retains high levels of expression throughout infection and elicits a dominant CD4$^+$
224 T cell response in C57BL/6 mice [11]. Due to the difficulty in obtaining large numbers of MHC
225 class II$^+$ cells from uninfected, RAG-1-deficient mice, we used TGPMs from age-matched, RAG-
226 1-deficient mice as a source of uninfected, inflammatory macrophages. We stained C7 or
227 TB10Rg3 T cells with 5uM of the proliferation dye eFluor450 (eBioscience) before co-culturing
228 them with the lung myeloid cells. After 72 hours, we measured the T cell proliferation as a marker
229 of T cell recognition. C7 T cells proliferated extensively when co-cultured with the infected lung
230 myeloid cells but not when co-cultured with uninfected TGPMs (Fig 4a, b). In contrast, TB10Rg3
231 T cells did not proliferate when co-cultured with the lung myeloid cells (Fig 4c, d). To assess
232 whether TB10Rg3 T cells could proliferate if TB10.4 was present, we pulsed the lung APCs with
233 the TB10.4$_{4-11}$ peptide for 1 hour before adding the TB10Rg3 T cells. As predicted, TB10Rg3 T
234 cells proliferated after 72 hours of co-culture with peptide-pulsed, lung myeloid cells (Fig 4c, d).
235 We considered the possibility that Mtb in lung myeloid cells may not grow well in vitro,
236 leading to altered antigen abundance that could affect T cell recognition. To address this
237 possibility, we measured the bacterial burden in the lung myeloid cells. There was a 3-fold
238 increase in the bacterial numbers between the beginning (d1) and the end (d4) of the experiment,
239 indicating that the bacteria remained viable (Fig 4e). Together, these data indicate that, under the
240 conditions in which C7 T cells recognized lung myeloid cells from Mtb-infected mice, TB10Rg3 T

241 cells did not recognize these lung myeloid cells.

242

243 **TB10Rg3 CD8$^+$ and P25 CD4$^+$ T cells recognize macrophages infected with TB10.4-**

244 **or Ag85b-expressing Listeria.**

245 We next investigated whether the location of the antigen might affect the presentation of
246 TB10.4 since the MHC class I antigen presentation pathway primarily samples the cytosol,
247 whereas Mtb is a classic phagosomal pathogen. TB10.4-specific CD8$^+$ T cells are primed and
248 expanded during Mtb infection, so the TB10.4 antigens must be cross-presented; however,
249 whether Mtb-infected macrophages can competently cross-present mycobacterial antigens is
250 unknown. We investigated these possibilities using ΔLLO or ΔActA mutant strains of *Listeria*
251 *monocytogenes* engineered to express the full length TB10.4 protein, hereafter referred to as
252 ΔLLO.TB10.4 or ΔActA.TB10.4, respectively. Both are attenuated strains: the ΔLLO.TB10.4
253 mutant cannot escape from the vacuole, while the ΔActA.TB10.4 mutant can escape from the
254 vacuole but not from the cell. Hence, the TB10.4 protein made by the ΔLLO.TB10.4 strain will
255 remain trapped in the phagosome, but the TB10.4 protein made by the ΔActA.TB10.4 strain will
256 gain access to the cytosol.

257 TB10Rg3 T cells recognized ΔActA.TB10.4-infected TGPMs based on an increased
258 frequency of Nur77-expressing cells ($p<0.005$) and the Nur77 MFI of all TB10Rg3 T cells
259 ($p<0.005$) (Fig 5a-c). Bafilomycin, which inhibits vacuolar acidification and impairs the entry of the
260 ΔActA.TB10.4 strain into the cytosol, diminished the frequency of Nur77-expressing cells
261 ($p<0.005$) and Nur77 MFI ($p<0.01$) (Fig 5a, top, b, c). In contrast, TB10Rg3 T cells co-cultured
262 with ΔLLO.TB10.4-infected TGPMs showed no increase in the frequency of Nur77-expressing
263 cells or the Nur77 MFI (Fig 5a bottom, d, e). If recombinant listeriolysin (rLLO), the protein missing
264 from the ΔLLO.TB10.4 strain, was added to the infected macrophages, an increase in the
265 frequency of Nur77-expressing TB10Rg3 T cells ($p<0.01$) and the Nur77 MFI ($p<0.01$) became

266 apparent. We also determined whether P25 T cells recognized Ag85b-expressing *Listeria*
267 *monocytogenes* using the recombinant Listeria strains ΔActA.Ag85b and ΔLLO.Ag85b. Based on
268 the propensity of MHC class II to present extracellular and vacuolar antigens, P25 cells
269 recognized TGPMs infected with either ΔActA.Ag85b or ΔLLO.Ag85b, based on an increase in
270 the frequency of Nur77-expressing T cells and Nur77 MFI ($p<0.005$) (Fig 5g, h). These results
271 show that 1) TGPMs can efficiently process the full length TB10.4 protein and present the
272 TB10.4_{4-11} epitope via MHC class I; 2) this process is more efficient when the bacteria are in the
273 cytosol; and 3) TB10Rg3 T cells can efficiently recognize TB10.4_{4-11} presented during a live
274 infection.
275

276 **TB10.4-specific $CD8^+$ T cells do not recognize Mtb overexpressing TB10.4.**

277 We considered several additional possibilities as to why the TB10Rg3 T cells did not
278 recognize Mtb-infected macrophages. Antigen abundance can affect T cell recognition, so we
279 next tested whether increasing the level of TB10.4 protein expression might enhance TB10Rg3 T
280 cell recognition of Mtb-infected macrophages. Since Mtb secretes esxH (TB10.4) together with
281 esxG as a heterodimer [35], we developed a recombinant strain of H37Rv (esxGH-OE.Mtb), which
282 overexpresses both esxG and esxH under the control of a tet^{ON} promoter. After tetracycline
283 induction for 24 hours, the esxG and esxH mRNA expression increased multiple folds (Fig 6a).
284 Prior to in vitro infection, we treated esxGH-OE.Mtb with or without tetracycline. The next day,
285 TGPMs were infected with induced or uninduced esxGH-OE.Mtb. P25 T cells produced similar
286 amounts of IFNγ when co-cultured with macrophages infected with either uninduced or induced
287 esxGH-OE.Mtb, which was expected since Ag85b expression should not be altered (Fig 6b).
288 Despite increasing the production of TB10.4 by Mtb, TB10Rg3 T cells still did not recognize Mtb-
289 infected macrophages (Fig 6c). Although we cannot be certain that the induction of EsxGH leads
290 to an increased amount of antigen delivered to the antigen processing pathway, this result

291 suggests that antigen abundance is not limiting TB10.4-specific $CD8^+$ T cell recognition of Mtb-
292 infected macrophages.
293

294 **Mtb infection does not significantly impair MHC class I and II expression by**
295 **macrophages.**

296 We also investigated whether Mtb may inhibit MHC class I expression by infected TGPMs.
297 Mtb and TLR2 agonists inhibit IFNγ-induced MHC class II expression by bone marrow derived
298 macrophages, and the mycobacterial PPE38 protein can inhibit MHC class I expression in
299 RAW264.7 macrophages and TGPMs infected with *Mycobacterium smegmatis* [36, 37].
300 Therefore, we asked whether Mtb impaired MHC class I expression in our in vitro infection system,
301 especially since the TGPMs were not pre-activated with IFNγ prior to infection. We measured
302 MHC class I and II expression by macrophages on each of the five days following infection. At
303 baseline, uninfected TGPMs expressed high MHC class I, and Mtb infection did not alter MHC
304 class I expression compared to the baseline (Fig 6d, e; solid lines). Although IFNγ pretreatment
305 of macrophages led to an increase in MHC class I expression in uninfected TGPMs, infected
306 TGPMs did not achieve the same peak levels (Fig 6d, e; dotted lines). As expected, the regulation
307 of MHC class II was more sensitive to IFNγ. Uninfected TGPMs expressed low baseline levels of
308 MHC class II (Fig 6f, g; solid lines). IFNγ pretreatment resulted in a >100-fold increase in MHC
309 class II median fluorescence intensity (MFI) in the uninfected TGPMs, which peaked on day 3
310 with a >2000-fold increase over the baseline (Fig 6f, g; dotted lines). Mtb-infection alone did not
311 significantly affect MHC class II expression, and consistent with previous studies, Mtb significantly
312 impaired the induction of MHC class II by IFNγ pretreatment (Fig 6f, g). These data show that, in
313 our in vitro infection model where the TGPMs were unstimulated, Mtb infection did not inhibit class
314 I and II MHC expression. Importantly, the differences in MHC class I or class II expression by
315 Mtb-infected macrophages cannot explain why P25 T cells, but not TB10Rg3 T cells, recognized

316 infected macrophages.

317

318 **Macrophages cross-present antigens from non-viable Mtb to TB10.4-specific CD8$^+$**

319 **T cells.**

320 Next, we hypothesized that Mtb may interfere with MHC class I presentation of

321 mycobacterial antigens. Therefore, we tested the ability of the P25 and TB10Rg3 T cell lines to

322 recognize TGPMs cultured with γ-irradiated, nonviable Mtb. Activation of pattern recognition

323 receptors such as TLR2 and TLR4 by large amounts of dead bacteria might induce large amounts

324 of IL-12 and IL-18, resulting in cytokine-driven T cell activation. Taking this concern into

325 consideration, we used MHC-mismatched TGPMs as a control. We pulsed macrophages with a

326 dose titration of γ-irradiated Mtb, then added TB10Rg3 or P25 T cells, and measured IFNγ

327 secretion by the T cells after 72 hours. Both P25 and TB10Rg3 T cells produced high amounts of

328 IFNγ when cultured with MHC-matched (i.e., H-2^b) but not with MHC-mismatched (i.e., H-2^k)

329 TGPMs, and this response was dose dependent (Fig 6h, i). The ability of macrophages to process

330 and present TB10.4 after phagocytosing γ-irradiated Mtb but not viable bacteria raises the

331 possibility that live Mtb actively inhibit MHC class I presentation of TB10.4.

332

333 **Polyclonal, TB10.4$_{4\text{-}11}$-tetramer negative CD8$^+$ T cells from the lungs of Mtb-infected**

334 **mice recognize infected macrophages.**

335 Along with the previous finding that TB10.4$_{4\text{-}11}$-specific CD8$^+$ T cells make up ~40% of total

336 lung CD8$^+$ T cells during infection (S1 Figure) [19], our finding that TB10Rg3 T cells do not

337 recognize Mtb-infected macrophages suggests that TB10.4 may be a decoy antigen. This raises

338 the question whether the inability to recognize Mtb-infected macrophages is a general feature of

339 the CD8$^+$ T cell response to Mtb, or if this is a unique feature of TB10.4-specific CD8$^+$ T cells.

340 Therefore, we determined whether polyclonal CD8$^+$ T cells from the lungs of infected mice could

341 recognize Mtb-infected macrophages. We carried out aerosol infection of C57BL/6 mice with
342 Erdman, and, 6-8 weeks post infection, we purified polyclonal $CD4^+$ or $CD8^+$ T cells from their
343 lungs and co-cultured them with Mtb-infected macrophages. After 72 hours of co-culture,
344 polyclonal $CD4^+$ T cells produced high amounts of IFNγ in a MHC-restricted manner (Fig 7a).
345 Interestingly, polyclonal $CD8^+$ T cells also produced IFNγ in a MHC-restricted manner when co-
346 cultured with Mtb-infected macrophages (Fig 7b). These results indicate that other antigen-
347 specific $CD8^+$ T cells recognizing Mtb-infected macrophages do exist, and infected TGPMs can
348 present Mtb antigens to $CD8^+$ T cells. However, based on the high abundance of TB10.4-specific
349 $CD8^+$ T cells post infection (S1 Figure), the non-TB10.4-specific, Mtb-specific $CD8^+$ T cells may
350 be dwarfed by the dominant TB10.4-specific $CD8^+$ T cells.

351 To better assess whether the IFNγ production by polyclonal $CD8^+$ T cells arose
352 predominantly from non-TB10.4-specific $CD8^+$ T cells, we used the TB10.$4_{4\text{-}11}$-tetramer to
353 separate TB10.4-specific and non-TB10.4-specific, polyclonal $CD8^+$ T cells from the lungs of
354 infected mice. After 72-hour co-culture with Mtb-infected macrophages, TB10.$4_{4\text{-}11}$-tetramer
355 negative $CD8^+$ (non-TB10.4-specific $CD8^+$) T cells produced significantly higher IFNγ compared
356 to that of uninfected control ($p<0.005$), and the production was MHC class I restricted (Fig 7c). In
357 contrast, TB10. $4_{4\text{-}11}$-specific $CD8^+$ T cells produced IFNγ in a non-MHC-restricted manner during
358 co-culture with both uninfected and Mtb-infected macrophages (Fig 7d). We cannot exclude the
359 possibility that the tetramer isolation might have inadvertently activated the TB10.$4_{4\text{-}11}$-specific
360 $CD8^+$ T cells. Nevertheless, these data show that polyclonal, TB10.$4_{4\text{-}11}$-tetramer negative $CD8^+$
361 T cells recognized Mtb-infected macrophages, supporting the notion of a subdominant T cell
362 response that may be effective at detecting Mtb.

363 ## Discussion

364 A complexity in defining T cell recognition is distinguishing cognate from non-cognate
365 recognition. T cell IFNγ production, a common readout for recognition, can be stimulated by IL-
366 12 and IL-18, two cytokines secreted by Mtb-infected cells [26, 28-30]. Even cognate recognition
367 does not always signify recognition of infected cells. Uninfected macrophages and dendritic cells
368 (DCs) can acquire exosomes, soluble proteins, apoptotic vesicles or necrotic debris containing
369 non-viable bacilli or its antigens, and present these to T cells [13, 38-40]. This detour pathway
370 allows T cells to be activated by uninfected DCs [38, 41]. Thus, T cell recognition of infected
371 macrophages, which is central to our fundamental paradigm of TB pathogenesis, remains poorly
372 defined.

373 Our study advances the understanding of T cell recognition of Mtb-infected cells. By
374 focusing on TCR-mediated recognition, our data show that T cells specific to immunodominant
375 antigens vary in their ability to recognize Mtb-infected macrophages. Despite being a persistent
376 and dominant population of $CD8^+$ T cells in the lungs of Mtb-infected mice, $TB10.4_{4-11}$-specific
377 $CD8^+$ T cells do not recognize Mtb-infected macrophages. While we primarily used TGPMs, which
378 have been used to model human macrophages [42, 43], we also showed that TB10.4-specific
379 $CD8^+$ T cells failed to recognize lung APCs from infected mice. Importantly, concurrent with our
380 analysis of $CD8^+$ T cells, we systematically assessed recognition of Mtb-infected macrophages
381 by Ag85b-specific (i.e., P25) and ESAT-6-specific (i.e., C7) $CD4^+$ T cells. Both recognized Mtb-
382 infected macrophages and inhibited bacterial growth (here and [10]). Thus, under conditions that
383 activated Mtb-specific $CD4^+$ T cells, no activation of TB10.4-specific $CD8^+$ T cells occurred. This
384 finding has many implications, among which the most important is that not all Mtb-specific T cells
385 recognize Mtb-infected macrophages.

386 These results led us to re-examine the evidence that $CD8^+$ T cells recognize infected cells.
387 In our evaluation of the literature, among the best evidence is: (1) direct ex vivo recognition of

388 Mtb-infected macrophages and DC by $CD4^+$ and $CD8^+$ T cells [44-47]; (2) murine T cells' cytolytic
389 activity (CTL) of MTb-infected cells [48-50]; (3) human $CD8^+$ T cells that recognize Mtb-infected
390 DC [51-53]. However, these data have limitations. The murine studies never demonstrated
391 cognate recognition, and the frequencies were lower than expected. The human studies only used
392 DC and not macrophages and used a high MOI, raising concerns about death of infected cells
393 and presentation of nonviable antigen. Nevertheless, these studies support the idea that $CD8^+$ T
394 cells recognize infected cells, but their frequency that recognize infected macrophages might be
395 lower than we previously expected. Such a finding might explain why $CD8^+$ T cells make a
396 disproportionately small contribution to host defense, even though Mtb infection elicits a robust
397 $CD8^+$ T cell response.

398 We investigated several mechanisms that might explain why TB10.4-specific $CD8^+$ T cells
399 do not recognize infected macrophages. One possibility is the access of the TB10.4 antigen to
400 the MHC class I processing pathway. Mtb can disrupt the phagosomal membrane and translocate
401 into the cytosol [54], though this action often occurs later in infection and leads to necrosis of the
402 macrophage [55]. We saw no evidence of recognition even at late time points such as days 4-5
403 post infection (Fig 3), when phagosomal disruption and bacterial translocation occurs [55]. The
404 importance of antigen location became apparent during the Listeria infection experiments, where
405 infected macrophages presented $TB10.4_{4\text{-}11}$ only when the bacteria could enter the cytosol (i.e.,
406 ΔActA.TB10 but not ΔLLO.TB10). The Listeria experiments also provided an additional insight.
407 Lindenstrom et al report that vaccination with TB10.4 (EsxH), which has a leucine at position 12
408 (i.e., IMYNYPAML), inefficiently generates TB10.4-specific $CD8^+$ T cells [56]. However,
409 vaccination with TB10.3 (EsxR), a related antigen that also contains the same epitope followed
410 by a methionine (i.e., IMYNYPAMM), elicits TB10.4-specific $CD8^+$ T cells. Based on that finding,
411 they conclude there is a processing defect that prevents the generation of the $TB10.4_{4\text{-}11}$ epitope
412 from the TB10.4 protein. However, they also find that TB10.4-specific $CD8^+$ T cells elicited by
413 TB10.3 vaccination recognize splenocytes pulsed with the rTB10.4 proteins, showing that the full

414 length TB10.4 protein can be processed and presented. These data indicate that the lack of
415 vaccine-elicited TB10.4-specific $CD8^+$ T cells is due to a problem with priming after vaccination
416 instead of an inability to process the IMYNYPAM epitope. Moreover, our data using TB10.4-
417 expressing Listeria show that TGPMs can process the full length TB10.4 protein and present the
418 $TB10.4_{4-11}$ epitope. Therefore, we conclude that amino acid sequence of TB10.4 does not hinder
419 its processing. The Listeria experiments also show the potential importance of antigen location
420 and raise the possibility that sequestration of the TB10.4 antigen in the phagosome renders it
421 inaccessible to the MHC class I presentation pathway.

422 Low antigen abundance could also explain the lack of recognition. We have previously
423 argued that there is limited amount of TB10.4 antigen presentation in the lungs of infected mice,
424 leading to extreme bias in the TCR repertoire of the TB10.4-specific $CD8^+$ T cell response and
425 defects in the memory-recall response in vivo [19, 23]. To test the possibility of low antigen
426 abundance, we overexpressed EsxG and EsxH (TB10.4) together but did not see greater T cell
427 recognition of Mtb-infected macrophages, suggesting that abundance might not be the issue.

428 Unexpectedly, macrophages pulsed with γ-irradiated Mtb were recognized by TB10.4-
429 specific $CD8^+$ T cells, raising the possibility that live Mtb actively inhibits MHC class I presentation
430 of TB10.4. This is particularly interesting since the presentation of CFP10, another ESAT-6-like
431 protein, by human DCs to $CD8^+$ T cells requires viable Mtb; DCs given heat-killed bacteria do not
432 present CFP10 to T cells [53]. While these data suggest that presentation requires active
433 secretion of CFP10 [57, 58], the heat-killing process could have destroyed CFP10, or there might
434 not have been sufficient amounts of CFP10 available in the non-viable bacteria. In combination
435 with our data showing polyclonal $CD8^+$ T cells recognize Mtb infected macrophages, these data
436 show that it is possible that certain antigens are presented by live Mtb while others are actively
437 prevented from being sampled by MHC class I.

438 Ag85b is an immunodominant antigen with an epitope recognized by $CD4^+$ T cells in
439 C57BL/6 mice. In vivo data shows that Ag85b-specific $CD4^+$ T cells can recognize Mtb-infected

440 cells early during infection; however, recognition decreases after infection is established [12, 14,
441 15, 59, 60]. The inability of Ag85b-specific $CD4^+$ T cells to efficiently recognize Mtb-infected bone-
442 marrow derived macrophages (BMDMs) or bone-marrow derived dendritic cells (BMDCs) stems
443 from a combination of reduced Ag85b expression by Mtb and because infected cells actively
444 export Ag85b into the extracellular milieu [12, 13]. In our experiments, we found that P25 T cells
445 recognized Mtb-infected macrophages and inhibited bacterial growth in a MHC-restricted manner.
446 A difference between the studies is the duration of macrophage and T cell co-culture. Grace et al
447 examined 16-24 hours and found a lack of recognition, whereas our assays focused on 72-96
448 hours and detected recognition. Moreover, it is unknown whether Mtb-infected cells still exported
449 antigens after the initial 24 hours of infection. Furthermore, the exported Ag85b could be taken
450 up by infected cells during longer co-cultures, leading to their recognition by T cells. Finally, it is
451 possible that cognate recognition of uninfected cells that present Ag85b could activate $CD4^+$ T
452 cells in a TCR-mediated manner, inducing IFNγ and indirectly controlling Mtb replication in
453 macrophages. Nonetheless, under conditions that activate Mtb-specific $CD4^+$ T cells, we could
454 not observe activation of TB10.4-specific $CD8^+$ T cells.

455 The $TB10.4_{4-11}$ epitope has been extensively used to characterize $CD8^+$ T cell responses
456 in the mouse model of TB, and TB10.4-specific $CD8^+$ T cell responses have also been
457 characterized in people with tuberculosis [19, 21, 23, 56, 61-63]. The finding that TB10.4-specific
458 $CD8^+$ T cells do not recognize infected macrophages was unexpected, particularly since TB10.4-
459 specific $CD8^+$ T cells persist in the lungs of infected mice and become more dominant with time
460 [18, 19]. From these experiments, two questions warrant further investigation: 1) whether the
461 $CD8^+$ T cells specific to other epitopes of TB10.4 also inefficiently recognize infected
462 macrophages, and 2) whether the species or the host genetic background influence recognition
463 of infected cells.

464 In retrospect, our findings may partially explain why eliciting TB10.4-specific $CD8^+$ T cells
465 by vaccination fails to protect mice against Mtb infection [23, 56]. While vaccination with

466 immunodominant antigens recognized by $CD4^+$ T cells (e.g., Ag85b, ESAT-6) induce moderate
467 protection [64, 65], we must consider the possibility that these antigens may not be the best
468 stimulators of protective immunity. Ag85b-specific $CD4^+$ T cells have variable efficacy, in large
469 part due to its reduced expression by the bacterium as early as 3 weeks after infection [11, 12].
470 However, by their nature, the recruitment of memory T cell responses specific for
471 immunodominant antigens is only incrementally faster than the primary T cell response [10, 23].
472 Thus, a crucial question for vaccine development is whether other Mtb antigens resemble TB10.4,
473 in that they elicit T cell responses that fail to recognize infected macrophages. We did detect
474 polyclonal $CD8^+$ T cells that recognized Mtb infected macrophages, corroborating a previous
475 study showing that polyclonal $CD8^+$ T cells from infected mice can lyse Mtb-infected cells [48].
476 These data indicate that there are antigens presented by Mtb-infected cells, even if those antigens
477 may be subdominant compared to TB10.4. Thus, future vaccine developments will benefit by
478 identifying antigen targets based on their ability of being presented rather than only their
479 immunogenicity.

480 Priming of TB10.4-specific $CD8^+$ T cells occurs early after Mtb infection in the lung draining
481 lymph node (LN) [23, 66]. Yet it is unknown whether priming of naïve T cells occurs via Mtb-
482 infected DCs, or uninfected DCs that acquire antigen through uptake of apoptotic blebs containing
483 Mtb proteins [38, 41], or by the transfer of antigen from cell to cell [40]. Priming by an uninfected
484 cell can have detrimental consequences if the infected cell presents a different repertoire of Mtb
485 antigens. Considering our findings, we propose that TB10.4 is a decoy antigen: TB10.4-specific
486 $CD8^+$ T cells expand in the LN during priming, accumulate in the lungs, but ineffectively recognize
487 Mtb-infected macrophages. This raises the hypothesis that not all immune responses elicited by
488 Mtb provide benefits to the host. Interestingly, Mtb genes encoding epitopes recognized by T cells
489 are more highly conserved than other DNA elements, implying that T cell recognition of these Mtb
490 epitopes may provide a survival advantage to the bacterium [67, 68]. For example, T cell
491 dependent inflammation may benefit Mtb by promoting transmission. Even though TB10.4 is more

492 variable than most other antigens, our results support these genetic data [67, 68]. Thus, Mtb
493 focuses the $CD8^+$ T cell response on the decoy antigen TB10.4 and distracts the immune
494 response from other antigens that might be targets of protective immunity, successfully evading
495 T cell immunity and enabling it to establish itself as persistent infection.

496 **Materials and Methods**
497
498 **Ethics Statement**

499 Studies involving animals were conducted following relevant guidelines and regulations,
500 and the studies were approved by the Institutional Animal Care and Use Committee at the
501 University of Massachusetts Medical School (Animal Welfare A3306-01), using the
502 recommendations from the Guide for the Care and Use of Laboratory Animals of the National
503 Institutes of Health and the Office of Laboratory Animal Welfare.

504 **Mice**

505 C57BL/6J, Rag-1-deficient (B6.129S7-Rag1^{tm1Mom}), B10 (C57BL/10J), B10.BR (B10.BR-
506 H2^{k2} H2-T18^{a}/SgSnJJrep), P25 (C57BL/6-Tg(H-2K^{b}-Tcrα,Tcrβ)P25Ktk/J) [24, 69], mice were
507 obtained from Jackson Laboratories (Bar Harbor, ME). C57BL/6J and B10 mice were used for
508 isolating MHC-matched TGPMs while B10.BR mice were used for isolating MHC-mismatched
509 TGPMs. C57BL/6 K$^{b-/-}$D$^{b-/-}$ (MHC I$^{-/-}$) mice were a generous gift from Dr. Kenneth Rock (University
510 of Massachusetts Medical School, MA). C7 TCR transgenic mice were a generous gift from Dr.
511 Eric Pamer (Memorial Sloan Kettering Cancer Center, NY)[34].

512 **Thioglycolate-elicited peritoneal macrophages**

513 Thioglycolate-elicited peritoneal macrophages were obtained 4-5 days after intra-
514 peritoneal injection of mice with 3% thioglycolate solution, as described [28]. 1×10^{5} macrophages
515 were plated per well. Macrophages were maintained in culture with RPMI 1640 media (Invitrogen
516 Life Technologies, ThermoFisher, Waltham, MA) supplemented with 10 mM HEPES, 1 mM
517 sodium pyruvate, 2 mM L-glutamine (all from Invitrogen Life Technologies) and 10% heat-
518 inactivated fetal bovine serum (HyClone, GE Healthcare Life Sciences, Pittsburgh, PA), referred
519 hereafter as supplemented complete media.

520 **Generation of CD8^{+} and CD4^{+} T cell lines**

521 Retrogenic mice expressing TB10Rg3 TCR specific for the TB10.4$_{4-11}$ epitope were

522 generated as previously described [19]. The TB10Rg3 $CD8^+$ T cells were isolated from these
523 mice, stimulated *in vitro* with irradiated splenocytes pulsed with the peptide $TB10.4_{4-11}$ in complete
524 media containing IL-2. P25 or C7 $CD4^+$ T cells were isolated from transgenic P25 or C7 mice,
525 respectively [24, 34]. The P25 and C7 cells were stimulated *in vitro* with irradiated splenocytes
526 pulsed with the $Ag85b_{241-256}$ peptide or the $ESAT\text{-}6_{1-15}$, respectively, in complete media containing
527 IL-2 and anti-IL-4. After the initial stimulation, these T cells were split every two days for 3-4
528 divisions and rested for two to three weeks. After the initial stimulation, the cells were cultured in
529 complete media containing IL-2 and IL-7.

530 **Peptides**

531 The following synthetic peptide epitopes were used as antigens: $TB10.4_{4-11}$
532 (IMYNYPAM); $Ag85b_{241-256}$ (QDAYNAAGGHNAVFN); and $ESAT\text{-}6_{1-15}$ (MTEQQWNFAGIEAAA).
533 We also generated a negative control peptide predicted to not bind to H-2 K^b: IMANAPAM. The
534 peptides were obtained from New England Peptides (Gardner, MA).

535 As positive controls assessing the function of macrophages to present antigen, uninfected
536 macrophages and, in certain experiments, infected macrophages were pulsed with the peptides
537 of interest. We pulsed macrophages by incubating 10uM of the peptides of interest with the
538 macrophages in supplemented complete RPMI 1640 media for 1 hour. After incubation, the cells
539 were washed 3 to 5 times with fresh supplemented complete RPMI 1640 media. The cells were
540 then resuspended in supplemented complete RPMI 1640 media for experiments.

541 ***In vitro* Mtb infection**

542 H37Rv was grown as previously described [28]. Bacteria was grown to an OD_{600} of 0.6 –
543 1.0, washed in RPMI, opsonized with TB coat (RPMI 1640, 1% heat-inactivated FBS, 2% human
544 serum, 0.05% Tween-80), washed again and filtered through a 5 micron filter to remove bacterial
545 clumps. The bacteria were counted using a Petroff-Hausser chamber. Infection was performed
546 as previously described [28]. The final multiplicity of infection (MOI), based on plating CFU, was

547 0.2-0.8 for all experiments. For CFU-based, bacterial growth inhibition assays, T cells were added
548 at a ratio of 5 T cells to each macrophage. Four replicate wells were used for each condition. Cell
549 cultures were lysed by adding 1/10th volume of with 10% Triton X-100 in PBS (final concentration
550 of 1%), and CFUs were determined by plating in serial dilutions of the lysates on Middlebrook
551 7H10 plates. CFUs were enumerated after culture for 21 days at 37°C and 5% CO_2.

552 ***In vivo* aerosol Mtb infection and lung cell isolation**

553 Aerosol infection of mice was done with the Erdman strain of Mtb using a Glas-Col aerosol-
554 generation device. A bacterial aliquot was thawed, sonicated for 1 minute and then diluted in 0.9%
555 NaCl-0.02% Tween-80 to 5 ml. The number of Mtb deposited in the lungs was determined for
556 each experiment, by plating undiluted lung homogenate from a subset of the infected mice within
557 24 hours of infection. The inoculum varied between 37-120 CFU. For the ex vivo APC
558 experiments, lung cells were isolated from Erdman-infected, RAG-1-deficient mice, 4-weeks post-
559 infection, and the APCs were enriched by positive selection using anti-MHC class II$^+$ microbeads
560 (Miltenyi Biotec, Bergisch Gladbach, Germany) and the Miltenyi AutoMACS. On average, the
561 isolated cells were 89% CD11c$^+$ or CD11c$^+$CD11b$^+$. The APCs were counted on a hemocytometer
562 and plated at 1x10^5 per well in supplemented complete RPMI 1640 media.

563 For the ex vivo CD4$^+$ and CD8$^+$ T cell experiments, single cell suspensions were isolated
564 from the lungs of infected C57BL/6 mice, 6 to 8 weeks post-infection, as described [10]. Polyclonal
565 CD4$^+$ and CD8$^+$ T cells were enriched by positive selection using Mouse CD4$^+$ and Mouse CD8$^+$
566 T cell isolation kits, respectively (Miltenyi Biotec). After enrichment, average purity for polyclonal
567 CD4$^+$ and CD8$^+$ T cells were 93% and 95%, respectively. For experiments investigating TB10.4$_{4-}$
568 $_{11}$-tetramer positive cells and polyclonal, non-TB10.4-specific, CD8$^+$ T cells, the following isolation
569 was done. Single cell suspensions from the lungs of infected mice were incubated with APC-
570 conjugated, TB10.4-$_{4-11}$-loaded, H-2^b tetramers from the National Institute of Health Tetramer
571 Core Facility (Emory University Vaccine Center, Atlanta, GA). Tetramer positive CD8$^+$ T cells were
572 then selected via the AutoMACS separator by anti-APC microbeads (Miltenyi Biotec). Average

573 purity of TB10.4_{4-11}-tetramer positive, $CD8^+$ T cells was 85%, with 1.4% contaminating $CD4^+$ T
574 cells. The tetramer negative population was subsequently washed and then enriched for
575 polyclonal $CD8^+$ T cells via Mouse $CD8^+$ T cell isolation kit (Miltenyi Biotec). Average purity of
576 polyclonal, non-TB10.4_{4-11}-tetramer positive, $CD8^+$ T cells was 75% with 0.8% contaminating
577 $CD4^+$ T cells and 13% contaminating TB10.4_{4-11}-tetramer positive $CD8^+$ T cells. The T cells were
578 counted using a hemocytometer and resuspended in supplemented complete RPMI 1640 media
579 before being used in experiments.

580 **Listeria infections**

581 The recombinant Listeria strains have been previously described [23]. For in vitro
582 infections, they were grown to an OD_{600} of 0.6-1.0 in BHI media (Sigma Aldrich) with 10 ug/ml
583 chloramphenicol (Sigma Aldrich) at 30°C. Macrophages were infected with the Listeria strains
584 using a MOI 50, for 45 minutes. Extracellular bacteria were eliminated by adding 60 ug/ml
585 gentamicin (Sigma Aldrich) for 20 minutes. Bacterial burden was assessed by lysing the infected
586 macrophages with 1% TritonX-100 in PBS, and plating serial dilutions of the lysate on BHI
587 agarose supplemented with 10ug/ml chloramphenicol (Sigma Aldrich, St. Louis, MO).
588 Recombinant listeriolysin (Prospec, East Brunswick, NJ) was added in some experiments at 2
589 ug/ml for 30 minutes, and any excess was washed away. Bafilomycin (InvivoGen, San Diego, CA)
590 was added in some experiments at 5 uM for 30 minute, before being washed away.

591 **Generation of TB10.4-overexpressing Mtb strains**

592 pJR1103 was cleaved with EcoRI-HF and SalI-HF [70]. mCherry preceded by the groEL2
593 promoter from H37Rv was inserted by HiFi Assembly. The resulting plasmid was cleaved with
594 NdeI and NotI-HF. The esxGH gene from H37Rv, along with 12 upstream nucleotides, was
595 inserted by HiFi Assembly following the plasmid-borne tetracycline-inducible promoter. All
596 enzymes used above were purchased from New England Biolabs. The resulting plasmid (pGB6)
597 was electroporated into Mtb H37Rv and integrated at the L5 site. RNA was purified from induced

598 and uninduced cultures using TRIzol (ThermoFisher) and chloroform extraction, followed by
599 purification on Zymo columns. cDNA was produced with Superscript IV (ThermoFisher), and
600 quantitative PCR was performed using the iTaq SYBR Green Supermix (Bio-Rad, Hercules, CA)
601 on an Applied Biosystems Viia 7 thermocycler.

602 **Irradiated H37Rv**

603 The following reagent was obtained through BEI Resources, NIAID, NIH: *Mycobacterium*
604 *tuberculosis*, Strain H37Rv, Gamma-Irradiated Whole Cells, NR-14819. The irradiated H37Rv
605 was gently sonicated using a cup-horn sonicator at a low power to disperse bacterial clumps while
606 limiting bacterial lysis. The number of bacteria were approximated by measuring the turbidity at
607 OD_{600}, and correlating it with live H37Rv (OD_{600} = 1 is equivalent to $3.0x10^8$ CFU/ml). To pulse
608 TGPMs, diluted, sonicated, γ-irradiated H37Rv were added to adherent macrophages for one
609 hour before repeatedly washing the cultures to remove residual extracellular bacteria.
610 Subsequently, TB10Rg3 or P25 T cells were added at a ratio of 1 T cell to 1 macrophages. After
611 72 hours, the amount of IFNγ in the supernatants was measured using Mouse IFNγ ELISA MAX
612 kits (Biolegend, San Diego, CA).

613 **Flow Cytometry Analysis**

614 The following cell surface antigens were detected by flow cytometry using the following
615 antibodies: mouse CD4 (clone GK1.5), CD8 (clone 53-6.7), CD3ε (clone 145-2C11), CD69 (clone
616 H1.2F3), I-A/I-E (clone M5/114.15.2), and H-$2K^b$ (clone AF6-88.5) (all from Biolegend). BV421-
617 and APC-conjugated, TB10.4_{4-11}-loaded, H-$2K^b$ tetramers were obtained from the National
618 Institutes of Health Tetramer Core Facility (Emory University Vaccine Center, Atlanta, GA).
619 Zombie Violet Fixable viability dye (Biolegend) or the Live/Dead Fixable Far Red Dead Cell stain
620 (ThermoFisher) were used for distinguishing live from dead cells. To stain for the Nur77
621 transcription factor, the Nur77 monoclonal antibody (clone 12.14) was used in combination with
622 the Foxp3 Transcription Factor Staining Buffer Set (both from ThermoFisher) by the

623 manufacturer's protocol. Live/dead viability staining and surface staining were done for 20
624 minutes at 4°C, and intracellular staining was done for 30 minutes at room temperature. Samples
625 were then fixed with 1% paraformaldehyde/PBS for 1 hour before being analyzed by a
626 MACSQuant flow cytometer (Miltenyi Biotec). FlowJo Software (Tree Star, Portland, OR) was
627 used to analyze the collected data. Single lymphocytes were gated by forward scatter versus
628 height and side scatter for size and granularity, and dead cells were excluded.

629 **Normalization and statistical analysis**

630 To compare the cellular expression of Nur77 and CD69 expression levels between time
631 points, the MFI values were normalized as follows: experimental values were divided by the
632 difference between the isotype control MFI (minimum response) and the peptide control MFI
633 (maximum response).

634 Each figure represents a minimum of 2 similar experiments, with 2 to 4 biological replicates
635 in each experiment. Data are represented as mean ± standard error of the mean (SEM). For
636 comparing two groups, a two-tailed, unpaired student's t-test was used. For more than two
637 groups, the data were analyzed using a one-way ANOVA. A p value < 0.05 was considered to be
638 statistically significant. Analysis was performed using GraphPad Prism, Ver. 7 (GraphPad
639 Software, La Jolla, CA).

640 ## Figure Legends:

641 **Figure 1. TB10.4-specific CD8+ (TB10Rg3) and Ag85b-specific CD4+ (P25) T cells both**
642 **recognize their cognate peptides.** (a) Representative histogram of Nur77 expression in P25 T
643 cells after 2 hours of co-culture with macrophages and (b) time course of Nur77 MFI in P25 T
644 cells. (c) Representative histogram of CD69 in P25 T cells after 2 hours of co-culture with
645 macrophages and (d) time course of CD69 MFI in P25 T cells. (e) Representative histogram of
646 Nur77 in TB10Rg3 T cells after 2 hours of co-culture and (f) time course of Nur77 MFI in TB10Rg3
647 T cells. (g) Representative histogram of CD69 in TB10Rg3 T cells at 2 hours of co-culture with
648 macrophages and (h) time course of CD69 MFI in TB10Rg3 T cells. (i) CD69 MFI and (j) IFNγ
649 production by P25 T cells after 72 hours of co-culture. (k) CD69 MFI and (l) IFNγ production by
650 TB10Rg3 cells after 72 hours of co-culture. MFI, mean fluorescence intensity; mφ, macrophage.
651

652 **Figure 2. Ag85b-specific CD4$^+$ T cells, but not TB10.4-specific CD8$^+$ T cells, inhibit bacterial**
653 **growth *in vitro*.** (a) Matched (H-2^b) or mismatched (H-2^k) macrophages were infected with H37Rv
654 for 2 hours, and then, one day post-infection, T cells were added. Separately, TB10.4 or Ag85b
655 peptide was added to Mtb-infected (H-2^b) macrophages, and then T cells were added. CFU were
656 determined 4 days later. (b) C57BL/6 macrophages were infected with H37Rv as described
657 above. The next day, TB10.4 or Ag85B peptide was added to selected wells. TB10Rg3,
658 TB10RgP, TB10RgL, TB10RgR, or P25 T cells, were added, and CFUs were determined 4 days
659 later. Results are representative of at least three experiments. Statistical testing was by one-way
660 ANOVA, using the Dunnett posttest compared to d5. *, #, $p<0.05$; **, $p<0.01$; ***, $p<0.005$; ****,
661 $p<0.0001$.
662

663 **Figure 3. Ag85b-specific CD4$^+$ T cells, but not TB10.4-specific CD8$^+$ T cells, recognize Mtb-**
664 **infected macrophages.** (a-d) T cells were co-cultured with peptide-pulsed, Mtb-infected, or

665 uninfected macrophages for 2 hours. (a) Representative histogram of Nur77 expression in P25 T
666 cells and the normalized Nur77 MFI. (b) Representative histogram of CD69 expression in P25 T
667 cells and the normalized CD69 MFI. (c) Representative histogram of Nur77 in TB10Rg3 T cells
668 and the normalized Nur77 MFI. (d) Representative histogram of CD69 expression in TB10Rg3 T
669 cells and the normalized CD69 MFI. (e-f) TB10Rg3 T cells were co-cultured with uninfected,
670 peptide-pulsed, or Mtb-infected macrophages for 2 hours on d1, d3, and d5 post infection.
671 Normalized expression of (e) Nur77 or (f) CD69 by TB10Rg3 T cells. P25 (g) or TB10Rg3 (h) T
672 cells were co-cultured with uninfected, peptide-pulsed, or Mtb-infected macrophages, and IFNγ
673 production was measured after 72 hours. (i) TB10Rg3, TB10RgP, TB10RgL, TB10RgR, or P25 T
674 cells were cultured with uninfected, Mtb-infected, or peptide-pulsed macrophages. After 3 days,
675 IFNγ in the supernatants was measured. Figures are representative of at least 5 (a-d, TB10Rg3),
676 2 (a-d, P25), 3 (e-h), or 2 (i) experiments. Statistical analysis was done by one-way ANOVA with
677 Dunnett posttest (a-d) or two-way ANOVA with Sidak posttest (g-h). *, $p<0.05$; **, $p<0.01$; and ***,
678 $p<0.005$.
679
680 **Figure 4. TB10Rg3 CD8$^+$ T cells do not recognize lung APCs from infected mice**. (a-d) T cell
681 proliferation after coculture with lung APC from infected mice, with or without cognate peptide, or
682 uninfected TGPM, based on eFluor450 fluorescence dilution after 72 hours. Representative flow
683 plot (a) and quantification (b) of C7 T cell proliferation. Representative flow plot (c) and
684 quantification (d) of TB10Rg3 T cell proliferation. (e) Bacterial burden in the lung APCs during *in*
685 *vitro* culture over the course of the experiment in the absence of T cells. Representative of 4
686 (TB10Rg3) or 2 (C7) experiments.
687
688 **Figure 5. TB10Rg3 and P25 T cells can recognize macrophages infected with *Listeria*
689 *monocytogenes* expressing TB10.4 and Ag85b proteins, respectively.** (a) Representative
690 flow plots showing Nur77 induction by TB10Rg3 T cells after co-culture with macrophages

691 infected with ΔActA.TB10 (top row) or ΔLLO.TB10 (bottom row) Listeria. (b) Analysis of the
692 frequency of Nur77-expressing TB10Rg3 T cells (b, d), or normalized MFI (c, e), after co-culture
693 with ΔActA.TB10 (b, c) or ΔLLO.TB10 (d, e) infected macrophages. (f) Representative flow plots
694 showing Nur77 induction by P25 population after co-culture with macrophages infected with
695 ΔActA.TB10 (top row) or ΔLLO.TB10 (bottom row) Listeria. (g) Analysis of the frequency of Nur77-
696 expressing P25 T cells and (h) normalized MFI of P25 T cells. Representative of at least two
697 experiments. Statistical testing by one-way ANOVA with Dunnett posttest. *, $p<0.05$; **, $p<0.01$;
698 and ***, $p<0.005$.
699
700 **Figure 6. Probing potential mechanisms for lack of recognition by TB10Rg3 T cells.** (a-c)
701 EsxG (TB10.4) and its partner EsxH were overexpressed together in H37Rv to determine whether
702 increasing TB10.4 abundance would lead to recognition of infected macrophages (esxGH-
703 OE.Mtb). (a) Tetracycline treatment of esxGH-OE.Mtb in broth culture induces esxG and esxH,
704 but not fbpB and sigA, mRNA as measured by qPCR. Fold-induction was normalized to baseline
705 (i.e., uninduced). IFNγ production by (b) P25 or (c) TB10Rg3 T cells after co-culture with
706 macrophages infected with uninduced or induced esxGH-OE.Mtb. (d-g) MHC class I and II
707 expression by Mtb infected-macrophages. Representative histograms (d, f) and (e, g) fold-change
708 of MHC class I (d, e) or class II (f, g) expression on infected cells. (h) P25 and (i) TB10Rg3
709 production of IFNγ after co-culture with macrophages pulsed with titrated amounts of γ-irradiated
710 (non-viable) H37Rv. Data is representative of 3 experiments. Statistical testing by one-way
711 ANOVA with Dunnett posttest. *, $p<0.05$; **, $p<0.01$; and ***, $p<0.005$.
712
713 **Figure 7. Polyclonal $CD8^+$ T cells from the lungs of Mtb-infected mice recognize infected**
714 **macrophages.** IFNγ production by polyclonal $CD4^+$ (a) or $CD8^+$ (b) T cells after co-culture with
715 either MHC-matched ($H\text{-}2^b$) or MHC-mismatched ($H\text{-}2^k$), Mtb-infected macrophages. IFNγ

716 production by TB10.4_{4-11}-tetramer-depleted (c) or tetramer-enriched (d) polyclonal $CD8^+$ T cells
717 after co-culture with either MHC-matched (H-2^b) or MHC-mismatched (H-2^k), Mtb-infected
718 macrophages. Data is representative of at least 2 experiments. Statistical testing by a two-tailed,
719 unpaired Student's T test. *, $p<0.05$; **, $p<0.01$; and ***, $p<0.005$.
720

721 ## Supplemental Legends:

722 **S1 Supplemental Figure. TB10.$4_{4\text{-}11}$-tetramer positive $CD8^+$ dominates the pulmonary $CD8^+$**
723 **T cell response during Mtb infection in C57BL/6 mice.** Representative flow plot showing the
724 percent of TB10.$4_{4\text{-}11}$-tetramer positive $CD8^+$ T cells among lung cells isolated from mice infected
725 with Erdman via the aerosol route 6 weeks post-infection.

726

727 **S2 Supplemental Figure: TCR analysis and cloning of TCRs expressed by TB10.$4_{4\text{-}11}$-**
728 **specific $CD8^+$ T cells from the lungs of Mtb-infected C57BL/6 mice.**

729 Mononuclear lung cells were obtained from three individual C57BL/6 mice, 9 weeks after
730 low-dose aerosol infection with Mtb Erdman. Single TB10.$4_{4\text{-}11}$-tetramer$^+$ $CD8^+$ T cells from each
731 mouse were sorted into 96-well plates and the CDR3α and CDR3β sequences determined as
732 described [19]. The analysis of a representative mouse is shown, for which 141 CDR3α
733 sequences was determined. A clonal expansion of TB10.$4_{4\text{-}11}$-tetramer$^+$$CD8^+$ T cells, as
734 previously described [19], was suggested by the skewed distribution of TRAV and TRAJ families
735 (a), which shows an extreme bias in the use of TRAV7 and TRAJ15 gene segments, as well as a
736 dominant CDR3α amino acid (aa) length of 12 (b). (c) Analysis of all CDR3α aa sequence with a
737 length of 12 (n=112) identify a consensus motif of CAVSGGGRALIF for TB10.$4_{4\text{-}11}$-specific $CD8^+$
738 T cells.

739 Amplification of CDR3α and CDR3β sequences from the same well allowed pairing of
740 TCRα and TCRβ for individual TB10.$4_{4\text{-}11}$-specific $CD8^+$ T cells. Three individual mice were
741 analyzed in this manner (d). We identified an expanded CDR3β sequence containing the
742 "xDRENSD" motif, the same motif that had been previously defined by NexGen sequencing [19].
743 Thus, mouse L1 had an expansion of $CD8^+$ T cells with the CASSLDRENDYTF CDR3β sequence,
744 mouse L2 was dominated by $CD8^+$ T cells using the CDR3β sequence CASSQDRENDYTF, and
745 mouse L3 expressed two major expansions, one encoding CASSLDRENDYTF and the other,

746 CASSDDRENDYTF (d). Based on our ability to pair the CDR3α and CDR3β sequences, we
747 detected an interesting reciprocal conservation. Namely, the 'xDRENSD' CDR3β motif was
748 matched to a 'SxGGRA' CDR3α motif (e). Finally, we identified an expansion of a T cell clone in
749 mouse L1, which expressed a novel sequence that we had not previously observed (i.e.,
750 CASSPDRGNTGQLYF) (d, e). Thus, with a high degree of confidence, we paired the CDR3α and
751 CDR3β sequences belonging to 5 distinct TB10.$4_{4\text{-}11}$-specific $CD8^+$ T cell clones that had been
752 expanded in lungs of Mtb-infected C57BL/6 mice. The TCRα and TCRβ cDNAs were
753 reconstructed and cloned using standard methods, and retrogenic mice were subsequently
754 produced [19, 71, 72].
755
756 **S3 Supplemental Figure. Reconstitution and expression of specific TCRs in C57BL/6**
757 **retrogenic mice.**
758 Retrogenic mice were produced as previously described [19]. Six weeks after retroviral
759 transduction of bone marrow and reconstitution of congenically marked recipient mice, the
760 expression of the recombinant TCR was determined in peripheral blood. (a) The BW58$\alpha^-\beta^-$ cell
761 line was transduced with different retroviral constructs. GFP^+ cells were sorted three times, and
762 mAbs specific for Vα or Vβ were used to confirm successful TCR expression and pairing of
763 TB10RgP and TB10RgLD. The TB10Rg3 construct was included as internal control. (b)
764 Representative flow cytometry plots showed gating strategy of donor-derived GFP^+ specific $V\beta^+$
765 TB10.$4_{4\text{-}11}$-tetramer$^+$ $CD8^+$ TB10RgR and TB10RgLD mice. (c) Representative flow cytometry
766 plots of splenic T cells from TB10RgP retrogenic mice demonstrating $CD8^+GFP^+$ T cells staining
767 with the TB10.$4_{4\text{-}11}$-tetramer.
768
769

770 **Acknowledgements**

771 We would like to thank Dr. Kenneth Rock (University of Massachusetts Medical School,
772 MA) for the generous gift of C57BL/6 $K^{b-/-}D^{b-/-}$ (MHC $I^{-/-}$) mice. We thank Barry Kriegsman for
773 critical reading of the manuscript. We also thank the Animal Medicine team at University of
774 Massachusetts Medical School (Worcester, MA) for their technical assistance. This study was
775 funded by grants from the National Institutes of Health (R01 AI106725, R01 AI123286).

776

References:

1. Flynn JL, Chan J. Immune evasion by Mycobacterium tuberculosis: living with the enemy. Current Opinion in Immunology. 2003;15(4):450. doi: 10.1016/s0952-7915(03)00075-x.
2. Orme IM. Vaccines to prevent tuberculosis infection rather than disease: Physiological and immunological aspects. Tuberculosis (Edinb). 2016. doi: 10.1016/j.tube.2014.10.008. PubMed PMID: 25500316.
3. Behar SM, Carpenter SM, Booty MG, Barber DL, Jayaraman P. Orchestration of pulmonary T cell immunity during Mycobacterium tuberculosis infection: immunity interruptus. Semin Immunol. 2014;26(6):559-77. Epub 2014/10/15. doi: 10.1016/j.smim.2014.09.003. PubMed PMID: 25311810; PubMed Central PMCID: PMCPMC4250436.
4. Mogues T, Goodrich ME, Ryan L, LaCourse R, North RJ. The Relative Importance of T Cell Subsets in Immunity and Immunopathology of Airborne Mycobacterium tuberculosis Infection in Mice. The Journal of Experimental Medicine. 2001;193(3):271-80. doi: 10.1084/jem.193.3.271.
5. Pawlowski A, Jansson M, Skold M, Rottenberg ME, Kallenius G. Tuberculosis and HIV co-infection. PLoS Pathog. 2012;8(2):e1002464. Epub 2012/03/01. doi: 10.1371/journal.ppat.1002464. PubMed PMID: 22363214; PubMed Central PMCID: PMCPMC3280977.
6. Ginsberg AM, Ruhwald M, Mearns H, McShane H. TB vaccines in clinical development. Tuberculosis. 2016;99:S16-S20. doi: 10.1016/j.tube.2016.05.013.
7. Lindestam Arlehamn CS, Lewinsohn D, Sette A, Lewinsohn D. Antigens for CD4 and CD8 T cells in tuberculosis. Cold Spring Harb Perspect Med. 2014;4(7):a018465. Epub 2014/05/24. doi: 10.1101/cshperspect.a018465. PubMed PMID: 24852051; PubMed Central PMCID: PMCPMC4066646.
8. Pai M, Riley LW, Colford JM. Interferon-γ assays in the immunodiagnosis of tuberculosis: a systematic review. The Lancet Infectious Diseases. 2004;4(12):761-76. doi: 10.1016/s1473-3099(04)01206-x.
9. Srivastava S, Ernst JD. Cutting edge: Direct recognition of infected cells by CD4 T cells is required for control of intracellular Mycobacterium tuberculosis in vivo. J Immunol. 2013;191(3):1016-20. Epub 2013/07/03. doi: 10.4049/jimmunol.1301236. PubMed PMID: 23817429; PubMed Central PMCID: PMCPMC3725655.
10. Carpenter SM, Yang JD, Lee J, Barreira-Silva P, Behar SM. Vaccine-elicited memory CD4+ T cell expansion is impaired in the lungs during tuberculosis. PLoS Pathog. 2017;13(11):e1006704. Epub 2017/11/28. doi: 10.1371/journal.ppat.1006704. PubMed PMID: 29176787.
11. Moguche AO, Musvosvi M, Penn-Nicholson A, Plumlee CR, Mearns H, Geldenhuys H, et al. Antigen Availability Shapes T Cell Differentiation and Function during Tuberculosis. Cell Host Microbe. 2017;21(6):695-706 e5. doi: 10.1016/j.chom.2017.05.012. PubMed PMID: 28618268; PubMed Central PMCID: PMCPMC5533182.
12. Bold TD, Banaei N, Wolf AJ, Ernst JD. Suboptimal activation of antigen-specific CD4+ effector cells enables persistence of M. tuberculosis in vivo. PLoS Pathog. 2011;7(5):e1002063. Epub 2011/06/04. doi: 10.1371/journal.ppat.1002063. PubMed PMID: 21637811; PubMed Central PMCID: PMCPMC3102708.
13. Srivastava S, Grace PS, Ernst JD. Antigen Export Reduces Antigen Presentation and Limits T Cell Control of M. tuberculosis. Cell Host Microbe. 2016;19(1):44-54. Epub 2016/01/15. doi: 10.1016/j.chom.2015.12.003. PubMed PMID: 26764596; PubMed Central PMCID: PMCPMC4715867.
14. Lai R, Jeyanathan M, Afkhami S, Zganiacz A, Hammill JA, Yao Y, et al. CD11b(+) Dendritic Cell-Mediated Anti-Mycobacterium tuberculosis Th1 Activation Is Counterregulated by

826 CD103(+) Dendritic Cells via IL-10. J Immunol. 2018. Epub 2018/01/28. doi:
827 10.4049/jimmunol.1701109. PubMed PMID: 29374077.
828 15. Egen JG, Rothfuchs AG, Feng CG, Horwitz MA, Sher A, Germain RN. Intravital imaging
829 reveals limited antigen presentation and T cell effector function in mycobacterial granulomas.
830 Immunity. 2011;34(5):807-19. doi: 10.1016/j.immuni.2011.03.022.
831 16. Serafini A, Pisu D, Palu G, Rodriguez GM, Manganelli R. The ESX-3 secretion system is
832 necessary for iron and zinc homeostasis in Mycobacterium tuberculosis. PLoS One.
833 2013;8(10):e78351. Epub 2013/10/25. doi: 10.1371/journal.pone.0078351. PubMed PMID:
834 24155985; PubMed Central PMCID: PMCPMC3796483.
835 17. Griffin JE, Gawronski JD, Dejesus MA, Ioerger TR, Akerley BJ, Sassetti CM. High-
836 resolution phenotypic profiling defines genes essential for mycobacterial growth and cholesterol
837 catabolism. PLoS Pathog. 2011;7(9):e1002251. Epub 2011/10/08. doi:
838 10.1371/journal.ppat.1002251. PubMed PMID: 21980284; PubMed Central PMCID:
839 PMCPMC3182942.
840 18. Woodworth JS, Shin D, Volman M, Nunes-Alves C, Fortune SM, Behar SM.
841 Mycobacterium tuberculosis directs immunofocusing of CD8+ T cell responses despite
842 vaccination. J Immunol. 2011;186(3):1627-37. Epub 2010/12/24. doi:
843 10.4049/jimmunol.1002911. PubMed PMID: 21178003; PubMed Central PMCID:
844 PMCPMC3133636.
845 19. Nunes-Alves C, Booty MG, Carpenter SM, Rothchild AC, Martin CJ, Desjardins D, et al.
846 Human and Murine Clonal CD8+ T Cell Expansions Arise during Tuberculosis Because of TCR
847 Selection. PLoS Pathog. 2015;11(5):e1004849. Epub 2015/05/07. doi:
848 10.1371/journal.ppat.1004849. PubMed PMID: 25945999; PubMed Central PMCID:
849 PMCPMC4422591.
850 20. Skjot RLV, Brock I, Arend SM, Munk ME, Theisen M, Ottenhoff THM, et al. Epitope
851 Mapping of the Immunodominant Antigen TB10.4 and the Two Homologous Proteins TB10.3
852 and TB12.9, Which Constitute a Subfamily of the esat-6 Gene Family. Infection and Immunity.
853 2002;70(10):5446-53. doi: 10.1128/iai.70.10.5446-5453.2002.
854 21. Skjot RLV, Oettinger T, Rosenkrands I, Ravn P, Brock I, Jacobsen S, et al. Comparative
855 Evaluation of Low-Molecular-Mass Proteins from Mycobacterium tuberculosis Identifies
856 Members of the ESAT-6 Family as Immunodominant T-Cell Antigens. Infection and Immunity.
857 2000;68(1):214-20. doi: 10.1128/iai.68.1.214-220.2000.
858 22. Lewinsohn DA, Swarbrick GM, Park B, Cansler ME, Null MD, Toren KG, et al.
859 Comprehensive definition of human immunodominant CD8 antigens in tuberculosis. NPJ
860 Vaccines. 2017;2(1). doi: 10.1038/s41541-017-0008-6. PubMed PMID: 28775896; PubMed
861 Central PMCID: PMCPMC5538316.
862 23. Carpenter SM, Nunes-Alves C, Booty MG, Way SS, Behar SM. A Higher Activation
863 Threshold of Memory CD8+ T Cells Has a Fitness Cost That Is Modified by TCR Affinity during
864 Tuberculosis. PLoS Pathog. 2016;12(1):e1005380. Epub 2016/01/09. doi:
865 10.1371/journal.ppat.1005380. PubMed PMID: 26745507; PubMed Central PMCID:
866 PMCPMC4706326.
867 24. Tamura T, Ariga H, Kinashi T, Uehara S, Kikuchi T, Nakada M, et al. The role of
868 antigenic peptide in CD4+ T helper phenotype development in a T cell receptor transgenic
869 model. Int Immunol. 2004;16(12):1691-9. Epub 2004/10/13. doi: 10.1093/intimm/dxh170.
870 PubMed PMID: 15477229.
871 25. Moran AE, Holzapfel KL, Xing Y, Cunningham NR, Maltzman JS, Punt J, et al. T cell
872 receptor signal strength in Treg and iNKT cell development demonstrated by a novel fluorescent
873 reporter mouse. J Exp Med. 2011;208(6):1279-89. Epub 2011/05/25. doi:
874 10.1084/jem.20110308. PubMed PMID: 21606508; PubMed Central PMCID:
875 PMCPMC3173240.

876 26. Bastidas S, Graw F, Smith MZ, Kuster H, Gunthard HF, Oxenius A. CD8+ T cells are
877 activated in an antigen-independent manner in HIV-infected individuals. J Immunol.
878 2014;192(4):1732-44. Epub 2014/01/22. doi: 10.4049/jimmunol.1302027. PubMed PMID:
879 24446519.
880 27. Mariani F, Cappelli G, Riccardi G, Colizzi V. Mycobacterium tuberculosis H37Rv
881 comparative gene-expression analysis in synthetic medium and human macrophage. Gene.
882 2000. PubMed PMID: 10940566.
883 28. Rothchild AC, Jayaraman P, Nunes-Alves C, Behar SM. iNKT cell production of GM-
884 CSF controls Mycobacterium tuberculosis. PLoS Pathog. 2014;10(1):e1003805. Epub
885 2014/01/07. doi: 10.1371/journal.ppat.1003805. PubMed PMID: 24391492; PubMed Central
886 PMCID: PMCPMC3879349.
887 29. Okamoto I, Kohno K, Tanimoto T, Ikegami H, Kurimoto M. Development of CD8+
888 effector T cells is differentially regulated by IL-18 and IL-12. J Immunol. 1999;162(6):3202-11.
889 Epub 1999/03/27. PubMed PMID: 10092771.
890 30. Akdis M, Burgler S, Crameri R, Eiwegger T, Fujita H, Gomez E, et al. Interleukins, from 1
891 to 37, and interferon-gamma: receptors, functions, and roles in diseases. J Allergy Clin
892 Immunol. 2011;127(3):701-21 e1-70. Epub 2011/03/08. doi: 10.1016/j.jaci.2010.11.050.
893 PubMed PMID: 21377040.
894 31. Srivastava S, Ernst JD, Desvignes L. Beyond macrophages: the diversity of
895 mononuclear cells in tuberculosis. Immunological Reviews. 2014;262(1):179-92. doi:
896 10.1111/imr.12217.
897 32. Skold M, Behar SM. Tuberculosis Triggers a Tissue-Dependent Program of
898 Differentiation and Acquisition of Effector Functions by Circulating Monocytes. The Journal of
899 Immunology. 2008;181(9):6349-60. doi: 10.4049/jimmunol.181.9.6349.
900 33. Gonzalez-Juarrero M, Shim TS, Kipnis A, Junqueira-Kipnis AP, Orme IM. Dynamics of
901 Macrophage Cell Populations During Murine Pulmonary Tuberculosis. The Journal of
902 Immunology. 2003;171(6):3128-35. doi: 10.4049/jimmunol.171.6.3128.
903 34. Gallegos AM, Pamer EG, Glickman MS. Delayed protection by ESAT-6-specific effector
904 CD4+ T cells after airborne M. tuberculosis infection. J Exp Med. 2008;205(10):2359-68. Epub
905 2008/09/10. doi: 10.1084/jem.20080353. PubMed PMID: 18779346; PubMed Central PMCID:
906 PMCPMC2556792.
907 35. Ilghari D, Lightbody KL, Veverka V, Waters LC, Muskett FW, Renshaw PS, et al.
908 Solution structure of the Mycobacterium tuberculosis EsxG.EsxH complex: functional
909 implications and comparisons with other M. tuberculosis Esx family complexes. J Biol Chem.
910 2011;286(34):29993-30002. Epub 2011/07/07. doi: 10.1074/jbc.M111.248732. PubMed PMID:
911 21730061; PubMed Central PMCID: PMCPMC3191040.
912 36. Meng L, Tong J, Wang H, Tao C, Wang Q, Niu C, et al. PPE38 Protein of
913 Mycobacterium tuberculosis Inhibits Macrophage MHC Class I Expression and Dampens CD8+
914 T Cell Responses. Front Cell Infect Microbiol. 2017;7:68. Epub 2017/03/30. doi:
915 10.3389/fcimb.2017.00068. PubMed PMID: 28348981; PubMed Central PMCID:
916 PMCPMC5346565.
917 37. Noss EH, Harding CV, Boom WH. Mycobacterium tuberculosis inhibits MHC class II
918 antigen processing in murine bone marrow macrophages. Cell Immunol. 2000;201(1):63-74.
919 Epub 2000/05/12. doi: 10.1006/cimm.2000.1633. PubMed PMID: 10805975.
920 38. Winau F, Weber S, Sad S, de Diego J, Hoops SL, Breiden B, et al. Apoptotic vesicles
921 crossprime CD8 T cells and protect against tuberculosis. Immunity. 2006;24(1):105-17. Epub
922 2006/01/18. doi: 10.1016/j.immuni.2005.12.001. PubMed PMID: 16413927.
923 39. Smith VL, Cheng Y, Bryant BR, Schorey JS. Exosomes function in antigen presentation
924 during an in vivo Mycobacterium tuberculosis infection. Sci Rep. 2017;7:43578. Epub
925 2017/03/07. doi: 10.1038/srep43578. PubMed PMID: 28262829; PubMed Central PMCID:
926 PMCPMC5338015.

927 40. Srivastava S, Ernst JD. Cell-to-cell transfer of M. tuberculosis antigens optimizes CD4 T
928 cell priming. Cell Host Microbe. 2014;15(6):741-52. Epub 2014/06/13. doi:
929 10.1016/j.chom.2014.05.007. PubMed PMID: 24922576; PubMed Central PMCID:
930 PMCPMC4098643.
931 41. Schaible UE, Winau F, Sieling PA, Fischer K, Collins HL, Hagens K, et al. Apoptosis
932 facilitates antigen presentation to T lymphocytes through MHC-I and CD1 in tuberculosis. Nat
933 Med. 2003;9(8):1039-46. doi: 10.1038/nm906. PubMed PMID: 12872166.
934 42. Divangahi M, Chen M, Gan H, Desjardins D, Hickman TT, Lee DM, et al. Mycobacterium
935 tuberculosis evades macrophage defenses by inhibiting plasma membrane repair. Nat Immunol.
936 2009;10(8):899-906. Epub 2009/06/30. doi: 10.1038/ni.1758. PubMed PMID: 19561612;
937 PubMed Central PMCID: PMCPMC2730354.
938 43. Jayaraman P, Sada-Ovalle I, Nishimura T, Anderson AC, Kuchroo VK, Remold HG, et
939 al. IL-1beta promotes antimicrobial immunity in macrophages by regulating TNFR signaling and
940 caspase-3 activation. J Immunol. 2013;190(8):4196-204. Epub 2013/03/15. doi:
941 10.4049/jimmunol.1202688. PubMed PMID: 23487424; PubMed Central PMCID:
942 PMCPMC3622150.
943 44. Gonzalez-Juarrero M, Orme IM. Characterization of Murine Lung Dendritic Cells Infected
944 with Mycobacterium tuberculosis. Infection and Immunity. 2001;69(2):1127-33. doi:
945 10.1128/IAI.69.2.1127-1133.2001.
946 45. Bodnar KA, Serbina NV, Flynn JL. Fate of Mycobacterium tuberculosis within murine
947 dendritic cells. Infect Immun. 2001;69(2):800-9. Epub 2001/02/13. doi: 10.1128/IAI.69.2.800-
948 809.2001. PubMed PMID: 11159971; PubMed Central PMCID: PMCPMC97955.
949 46. Serbina NV, Flynn JL. Early emergence of CD8(+) T cells primed for production of type 1
950 cytokines in the lungs of Mycobacterium tuberculosis-infected mice. Infect Immun.
951 1999;67(8):3980-8. Epub 1999/07/23. PubMed PMID: 10417164; PubMed Central PMCID:
952 PMCPMC96683.
953 47. Nepal RM, Vesosky B, Turner J, Bryant P. DM, but not cathepsin L, is required to control
954 an aerosol infection with Mycobacterium tuberculosis. Journal of Leukocyte Biology.
955 2008;84(4):1011-8. doi: 10.1189/jlb.1207852.
956 48. Serbina NV, Liu CC, Scanga CA, Flynn JL. CD8+ CTL from lungs of Mycobacterium
957 tuberculosis-infected mice express perforin in vivo and lyse infected macrophages. J Immunol.
958 2000;165(1):353-63. Epub 2000/06/22. doi: 10.4049/jimmunol.165.1.353. PubMed PMID:
959 10861072.
960 49. Cowley SC, Elkins KL. CD4+ T cells mediate IFN-gamma-independent control of
961 Mycobacterium tuberculosis infection both in vitro and in vivo. J Immunol. 2003. PubMed PMID:
962 14568944.
963 50. Green AM, Difazio R, Flynn JL. IFN-gamma from CD4 T cells is essential for host
964 survival and enhances CD8 T cell function during Mycobacterium tuberculosis infection. J
965 Immunol. 2013;190(1):270-7. Epub 2012/12/13. doi: 10.4049/jimmunol.1200061. PubMed
966 PMID: 23233724; PubMed Central PMCID: PMCPMC3683563.
967 51. Caccamo N, Pietra G, Sullivan LC, Brooks AG, Prezzemolo T, La Manna MP, et al.
968 Human CD8 T lymphocytes recognize Mycobacterium tuberculosis antigens presented by HLA-
969 E during active tuberculosis and express type 2 cytokines. Eur J Immunol. 2015;45(4):1069-81.
970 doi: 10.1002/eji.201445193. PubMed PMID: 25631937.
971 52. Lewinsohn DA, Heinzel AS, Gardner JM, Zhu L, Alderson MR, Lewinsohn DM.
972 Mycobacterium tuberculosis-specific CD8+ T cells preferentially recognize heavily infected cells.
973 Am J Respir Crit Care Med. 2003;168(11):1346-52. Epub 2003/09/13. doi:
974 10.1164/rccm.200306-837OC. PubMed PMID: 12969871.
975 53. Lewinsohn DM, Zhu L, Madison VJ, Dillon DC, Fling SP, Reed SG, et al. Classically
976 restricted human CD8+ T lymphocytes derived from Mycobacterium tuberculosis-infected cells:

977 definition of antigenic specificity. J Immunol. 2001;166(1):439-46. Epub 2000/12/21. doi:
978 10.4049/jimmunol.166.1.439. PubMed PMID: 11123322.
979 54. van der Wel N, Hava D, Houben D, Fluitsma D, van Zon M, Pierson J, et al. M.
980 tuberculosis and M. leprae translocate from the phagolysosome to the cytosol in myeloid cells.
981 Cell. 2007;129(7):1287-98. Epub 2007/07/03. doi: 10.1016/j.cell.2007.05.059. PubMed PMID:
982 17604718.
983 55. Simeone R, Bobard A, Lippmann J, Bitter W, Majlessi L, Brosch R, et al. Phagosomal
984 rupture by Mycobacterium tuberculosis results in toxicity and host cell death. PLoS Pathog.
985 2012;8(2):e1002507. Epub 2012/02/10. doi: 10.1371/journal.ppat.1002507. PubMed PMID:
986 22319448; PubMed Central PMCID: PMCPMC3271072.
987 56. Lindenstrom T, Aagaard C, Christensen D, Agger EM, Andersen P. High-frequency
988 vaccine-induced CD8(+) T cells specific for an epitope naturally processed during infection with
989 Mycobacterium tuberculosis do not confer protection. Eur J Immunol. 2014. doi:
990 10.1002/eji.201344358. PubMed PMID: 24677089; PubMed Central PMCID:
991 PMCPMC4112357.
992 57. Grotzke JE, Siler AC, Lewinsohn DA, Lewinsohn DM. Secreted immunodominant
993 Mycobacterium tuberculosis antigens are processed by the cytosolic pathway. J Immunol.
994 2010;185(7):4336-43. Epub 2010/08/31. doi: 10.4049/jimmunol.1000801. PubMed PMID:
995 20802151; PubMed Central PMCID: PMCPMC2988655.
996 58. Woodworth JS, Fortune SM, Behar SM. Bacterial protein secretion is required for
997 priming of CD8+ T cells specific for the Mycobacterium tuberculosis antigen CFP10. Infect
998 Immun. 2008;76(9):4199-205. Epub 2008/07/02. doi: 10.1128/IAI.00307-08. PubMed PMID:
999 18591224; PubMed Central PMCID: PMCPMC2519428.
1000 59. Shafiani S, Tucker-Heard G, Kariyone A, Takatsu K, Urdahl KB. Pathogen-specific
1001 regulatory T cells delay the arrival of effector T cells in the lung during early tuberculosis. J Exp
1002 Med. 2010;207(7):1409-20. Epub 2010/06/16. doi: 10.1084/jem.20091885. PubMed PMID:
1003 20547826; PubMed Central PMCID: PMCPMC2901066.
1004 60. Egen JG, Rothfuchs AG, Feng CG, Winter N, Sher A, Germain RN. Macrophage and T
1005 cell dynamics during the development and disintegration of mycobacterial granulomas.
1006 Immunity. 2008;28(2):271-84. Epub 2008/02/12. doi: 10.1016/j.immuni.2007.12.010. PubMed
1007 PMID: 18261937; PubMed Central PMCID: PMCPMC2390753.
1008 61. Kamath A, Woodworth JS, Behar SM. Antigen-specific CD8+ T cells and the
1009 development of central memory during Mycobacterium tuberculosis infection. J Immunol.
1010 2006;177(9):6361-9. Epub 2006/10/24. doi: 10.4049/jimmunol.177.9.6361. PubMed PMID:
1011 17056567; PubMed Central PMCID: PMCPMC3133654.
1012 62. Elvang T, Christensen JP, Billeskov R, Thi Kim Thanh Hoang T, Holst P, Thomsen AR,
1013 et al. CD4 and CD8 T cell responses to the M. tuberculosis Ag85B-TB10.4 promoted by
1014 adjuvanted subunit, adenovector or heterologous prime boost vaccination. PLoS One.
1015 2009;4(4):e5139. Epub 2009/04/10. doi: 10.1371/journal.pone.0005139. PubMed PMID:
1016 19357780; PubMed Central PMCID: PMCPMC2663846.
1017 63. Billeskov R, Vingsbo-Lundberg C, Andersen P, Dietrich J. Induction of CD8 T cells
1018 against a novel epitope in TB10.4: correlation with mycobacterial virulence and the presence of
1019 a functional region of difference-1. J Immunol. 2007;179(6):3973-81. Epub 2007/09/06. doi:
1020 10.4049/jimmunol.179.6.3973. PubMed PMID: 17785835.
1021 64. Weinrich Olsen A, van Pinxteren LA, Meng Okkels L, Birk Rasmussen P, Andersen P.
1022 Protection of mice with a tuberculosis subunit vaccine based on a fusion protein of antigen 85b
1023 and esat-6. Infect Immun. 2001;69(5):2773-8. Epub 2001/04/09. doi: 10.1128/IAI.69.5.2773-
1024 2778.2001. PubMed PMID: 11292688; PubMed Central PMCID: PMCPMC98224.
1025 65. Brandt L, Elhay M, Rosenkrands I, Lindblad EB, Andersen P. ESAT-6 subunit
1026 vaccination against Mycobacterium tuberculosis. Infect Immun. 2000. PubMed PMID:
1027 10639447; PubMed Central PMCID: PMCPMC97206.

1028 66. Divangahi M, Desjardins D, Nunes-Alves C, Remold HG, Behar SM. Eicosanoid
1029 pathways regulate adaptive immunity to Mycobacterium tuberculosis. Nat Immunol.
1030 2010;11(8):751-8. Epub 2010/07/14. doi: 10.1038/ni.1904. PubMed PMID: 20622882; PubMed
1031 Central PMCID: PMCPMC3150169.
1032 67. Comas I, Chakravartti J, Small PM, Galagan J, Niemann S, Kremer K, et al. Human T
1033 cell epitopes of Mycobacterium tuberculosis are evolutionarily hyperconserved. Nat Genet.
1034 2010;42(6):498-503. Epub 2010/05/25. doi: 10.1038/ng.590. PubMed PMID: 20495566;
1035 PubMed Central PMCID: PMCPMC2883744.
1036 68. Coscolla M, Copin R, Sutherland J, Gehre F, de Jong B, Owolabi O, et al. M.
1037 tuberculosis T Cell Epitope Analysis Reveals Paucity of Antigenic Variation and Identifies Rare
1038 Variable TB Antigens. Cell Host Microbe. 2015;18(5):538-48. Epub 2015/11/27. doi:
1039 10.1016/j.chom.2015.10.008. PubMed PMID: 26607161; PubMed Central PMCID:
1040 PMCPMC4758912.
1041 69. Wolf AJ, Desvignes L, Linas B, Banaiee N, Tamura T, Takatsu K, et al. Initiation of the
1042 adaptive immune response to Mycobacterium tuberculosis depends on antigen production in the
1043 local lymph node, not the lungs. J Exp Med. 2008;205(1):105-15. Epub 2007/12/26. doi:
1044 10.1084/jem.20071367. PubMed PMID: 18158321; PubMed Central PMCID:
1045 PMCPMC2234384.
1046 70. Rock JM, Hopkins FF, Chavez A, Diallo M, Chase MR, Gerrick ER, et al. Programmable
1047 transcriptional repression in mycobacteria using an orthogonal CRISPR interference platform.
1048 Nature Microbiology. 2017;2:16274. doi: 10.1038/nmicrobiol.2016.274.
1049 71. Holst J, Szymczak-Workman AL, Vignali KM, Burton AR, Workman CJ, Vignali DA.
1050 Generation of T-cell receptor retrogenic mice. Nat Protoc. 2006;1(1):406-17. Epub 2007/04/05.
1051 doi: 10.1038/nprot.2006.61. PubMed PMID: 17406263.
1052 72. Bettini ML, Bettini M, Nakayama M, Guy CS, Vignali DA. Generation of T cell receptor-
1053 retrogenic mice: improved retroviral-mediated stem cell gene transfer. Nat Protoc.
1054 2013;8(10):1837-40. Epub 2013/09/07. doi: 10.1038/nprot.2013.111. PubMed PMID: 24008379;
1055 PubMed Central PMCID: PMCPMC3832243.
1056

Figure 1.

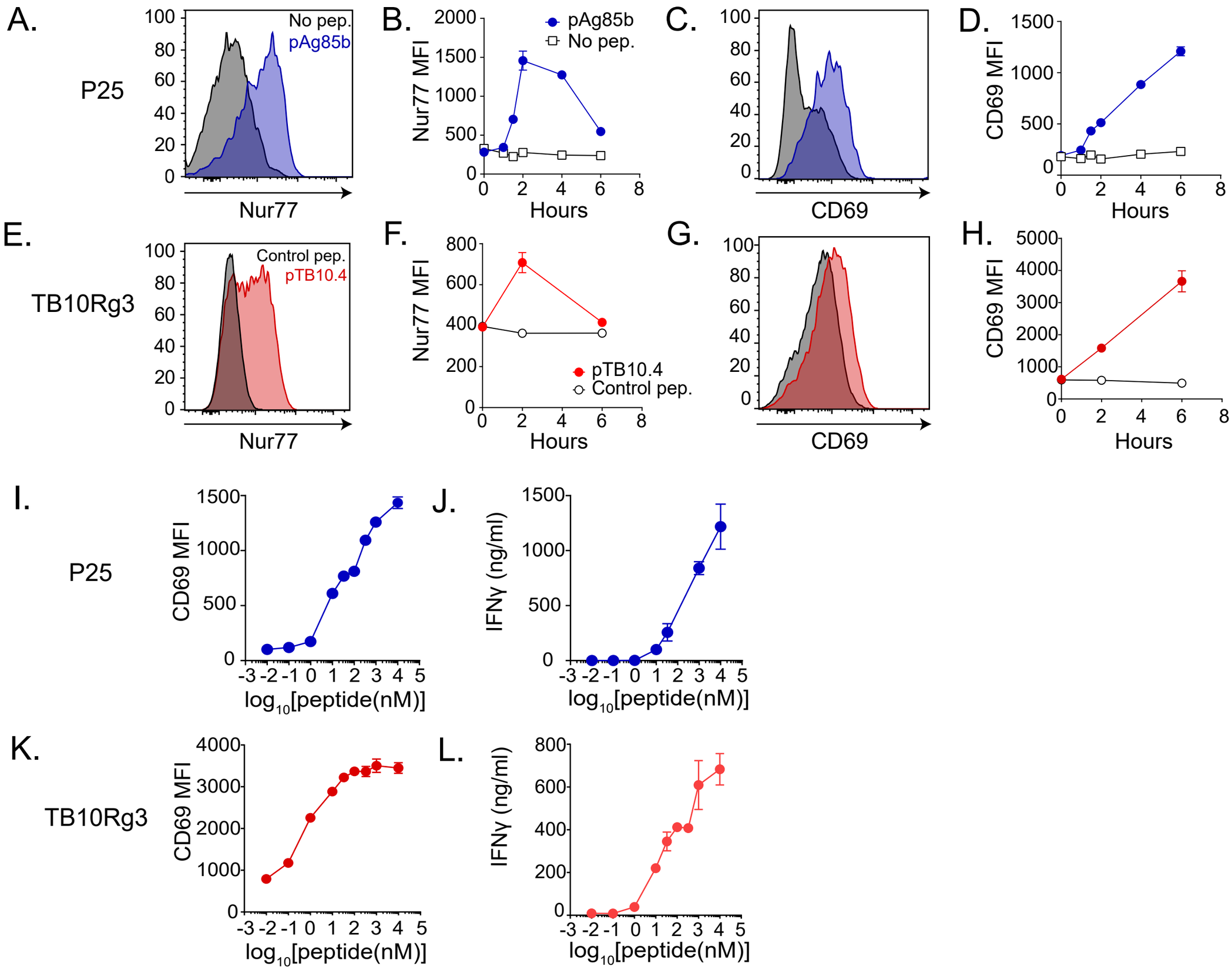
A.
P25
No pep.
pAg85b
Nur77
B.
pAg85b
No pep.
Nur77 MFI
Hours
C.
CD69
D.
CD69 MFI
Hours
E.
TB10Rg3
Control pep.
pTB10.4
Nur77
F.
Nur77 MFI
pTB10.4
Control pep.
Hours
G.
CD69
H.
CD69 MFI
Hours
I.
P25
CD69 MFI
log10[peptide(nM)]
J.
IFNγ (ng/ml)
log10[peptide(nM)]
K.
TB10Rg3
CD69 MFI
log10[peptide(nM)]
L.
IFNγ (ng/ml)
log10[peptide(nM)]

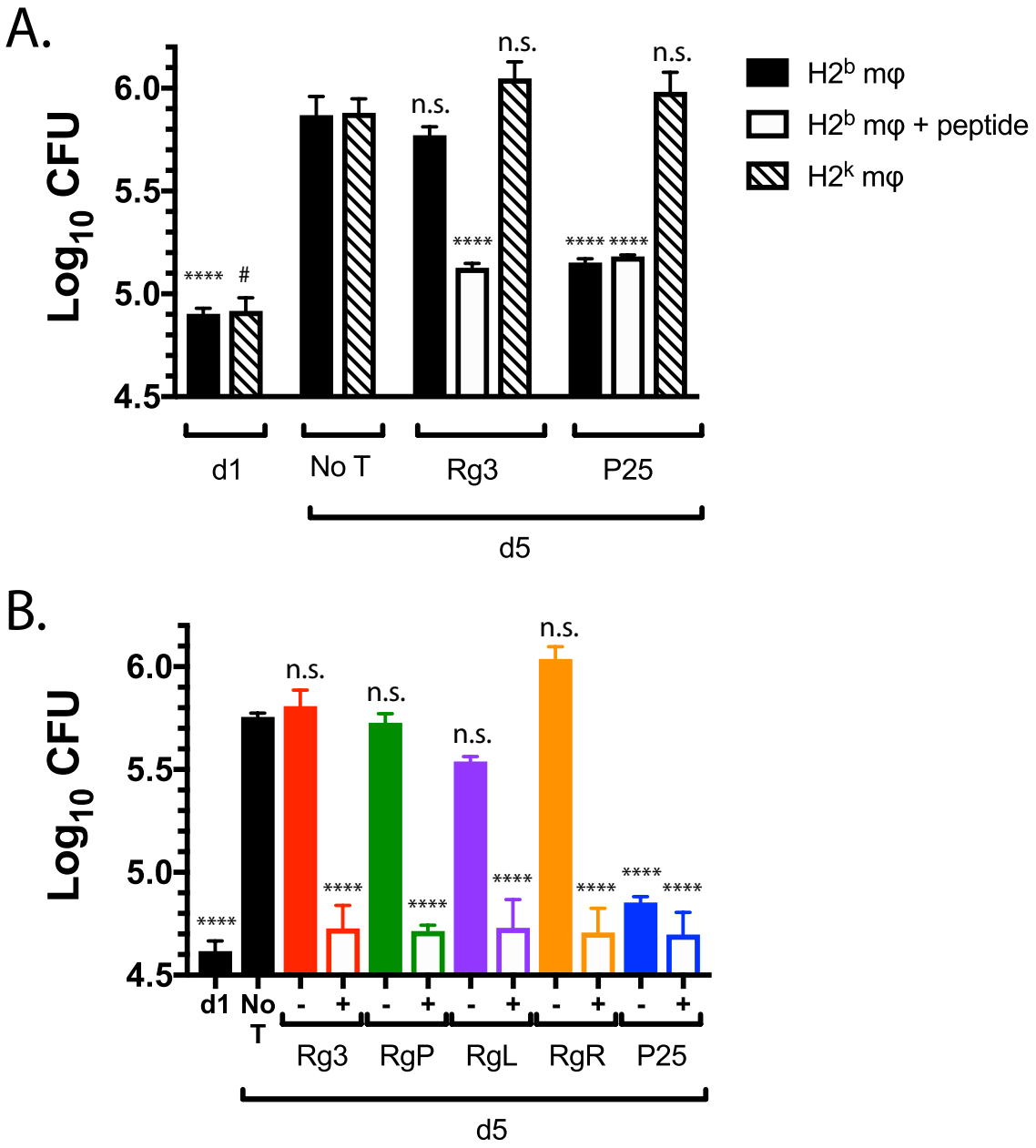
A.
Log10 CFU
6.0
5.5
5.0
4.5
****
#
n.s.
****
n.s.
****
****
n.s.
d1
No T
Rg3
P25
d5
H2b mφ
H2b mφ + peptide
H2k mφ
B.
Log10 CFU
6.0
5.5
5.0
4.5
****
n.s.
****
n.s.
****
n.s.
****
n.s.
****
****
****
d1
No T
-
+
Rg3
RgP
RgL
RgR
P25
d5

Figure 2.

Figure 3.

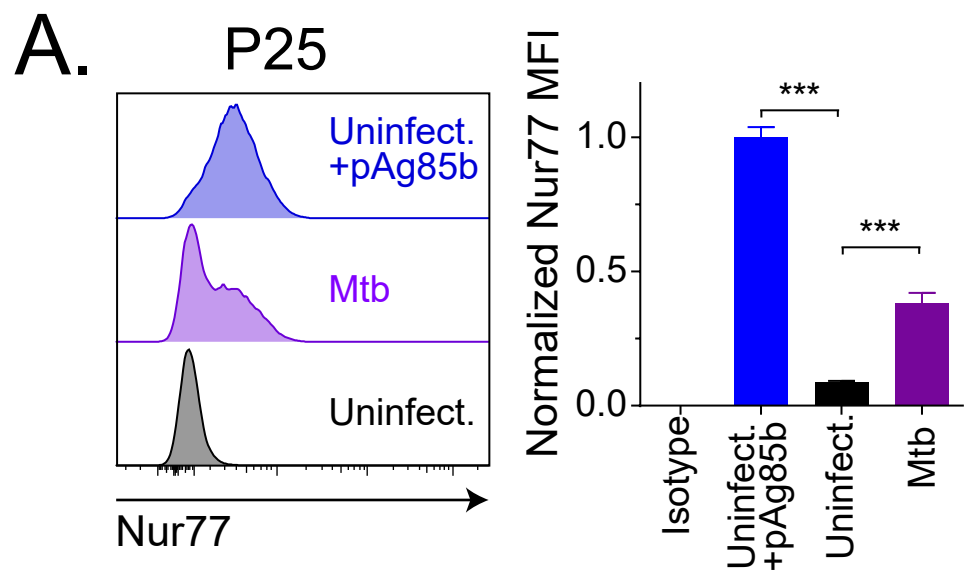
A.
P25
Uninfect. +pAg85b
Mtb
Uninfect.
Nur77
Normalized Nur77 MFI
1.0
0.5
0.0
***
***
Isotype
Uninfect. +pAg85b
Uninfect.
Mtb

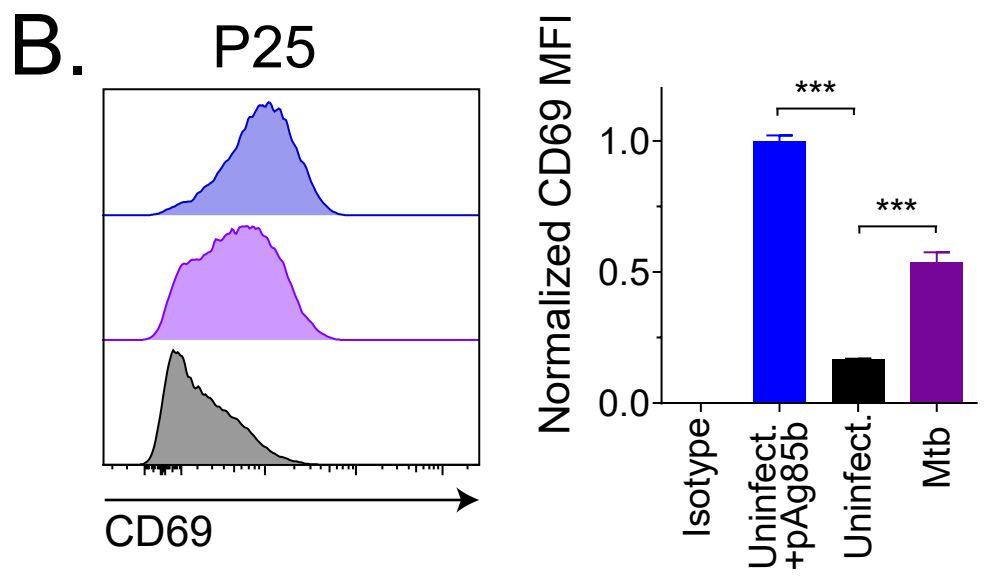
B.
P25
CD69
Normalized CD69 MFI
1.0
0.5
0.0
***
***
Isotype
Uninfect. +pAg85b
Uninfect.
Mtb

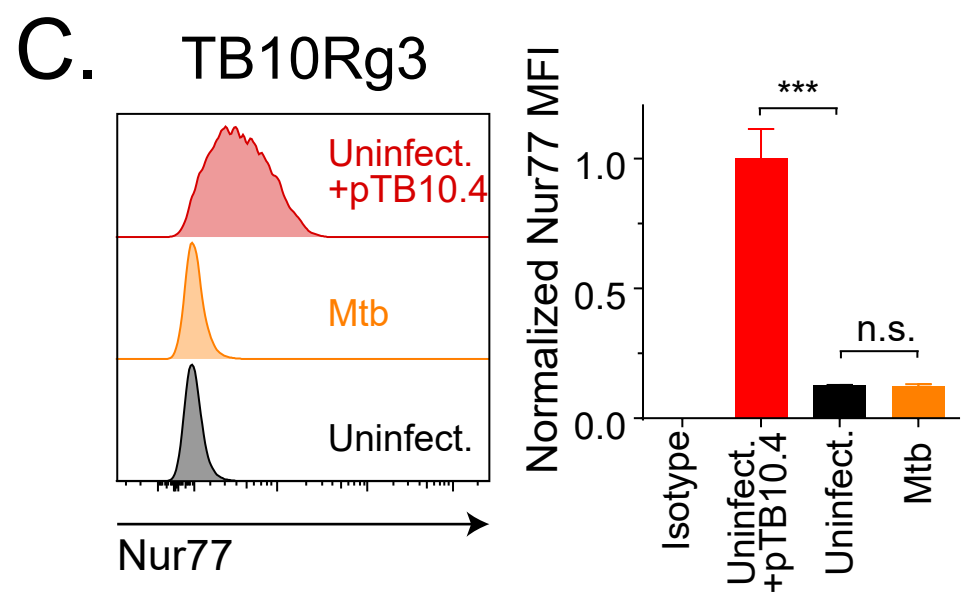
C.
TB10Rg3
Uninfect. +pTB10.4
Mtb
Uninfect.
Nur77
Normalized Nur77 MFI
1.0
0.5
0.0
***
n.s.
Isotype
Uninfect. +pTB10.4
Uninfect.
Mtb

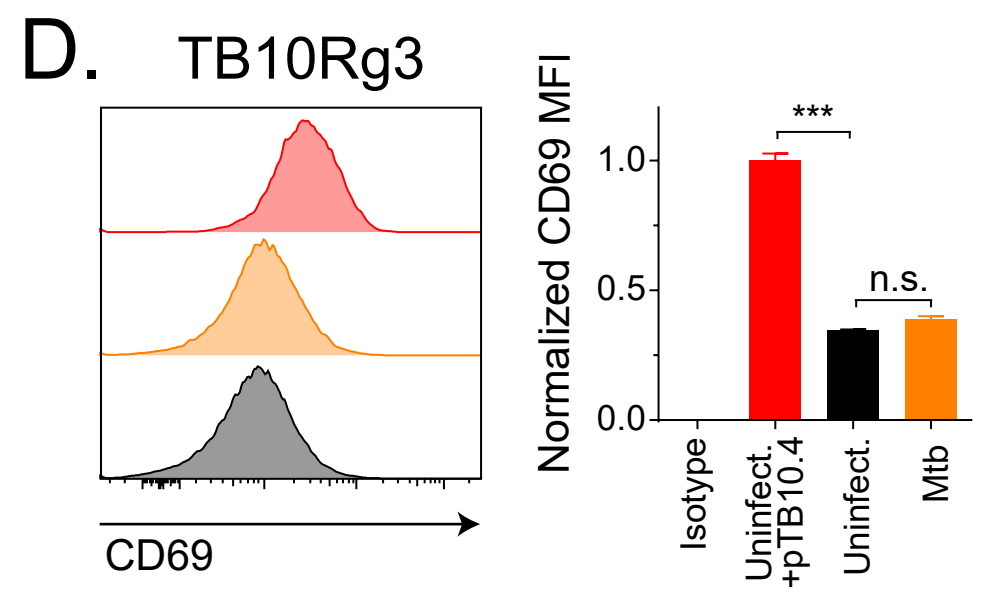
D.
TB10Rg3
CD69
Normalized CD69 MFI
1.0
0.5
0.0
***
n.s.
Isotype
Uninfect. +pTB10.4
Uninfect.
Mtb

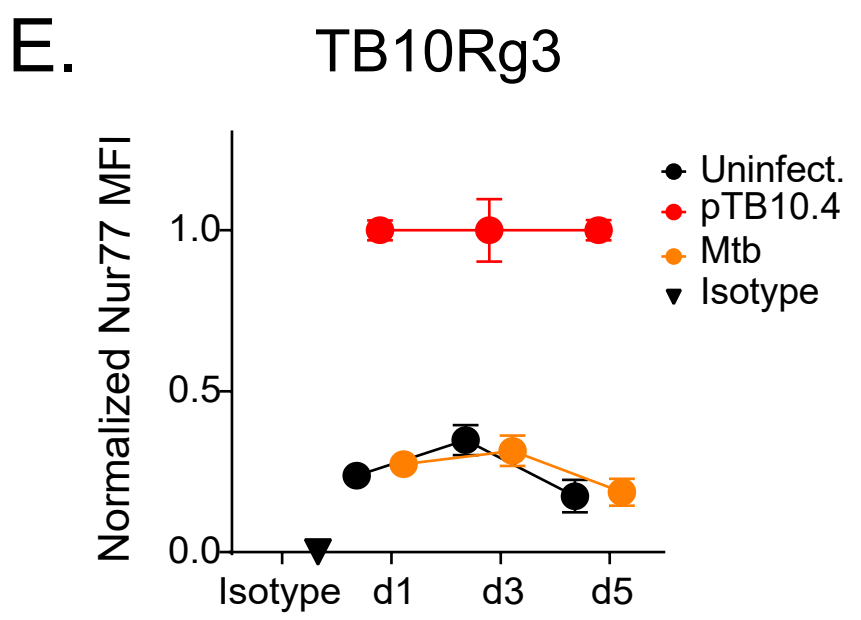
E.
TB10Rg3
Normalized Nur77 MFI
1.0
0.5
0.0
Uninfect.
pTB10.4
Mtb
Isotype
Isotype
d1
d3
d5

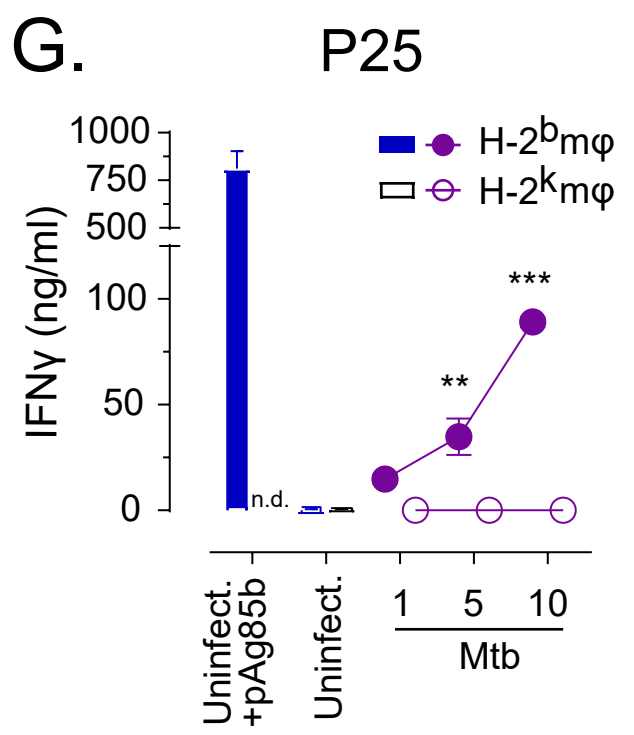
G.
P25
IFNγ (ng/ml)
1000
750
500
100
50
0
H-2bmφ
H-2kmφ
***
**
n.d.
Uninfect. +pAg85b
Uninfect.
1
5
10
Mtb

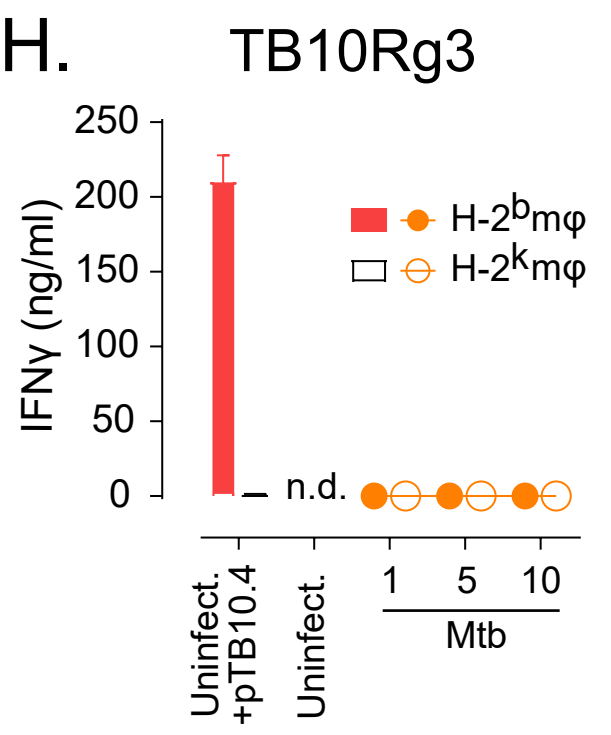
H.
TB10Rg3
IFNγ (ng/ml)
250
200
150
100
50
0
H-2bmφ
H-2kmφ
n.d.
Uninfect. +pTB10.4
Uninfect.
1
5
10
Mtb

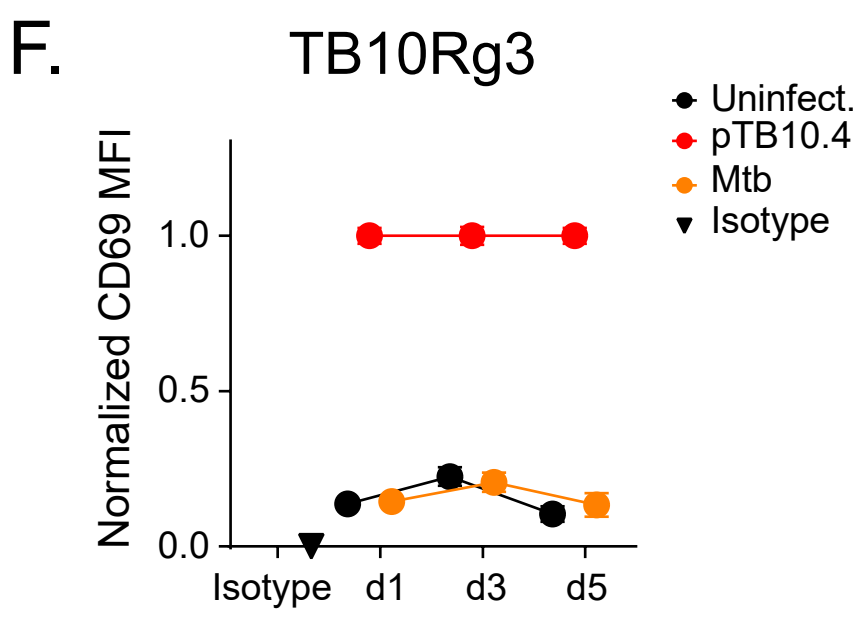
F.
TB10Rg3
Normalized CD69 MFI
1.0
0.5
0.0
Uninfect.
pTB10.4
Mtb
Isotype
Isotype
d1
d3
d5

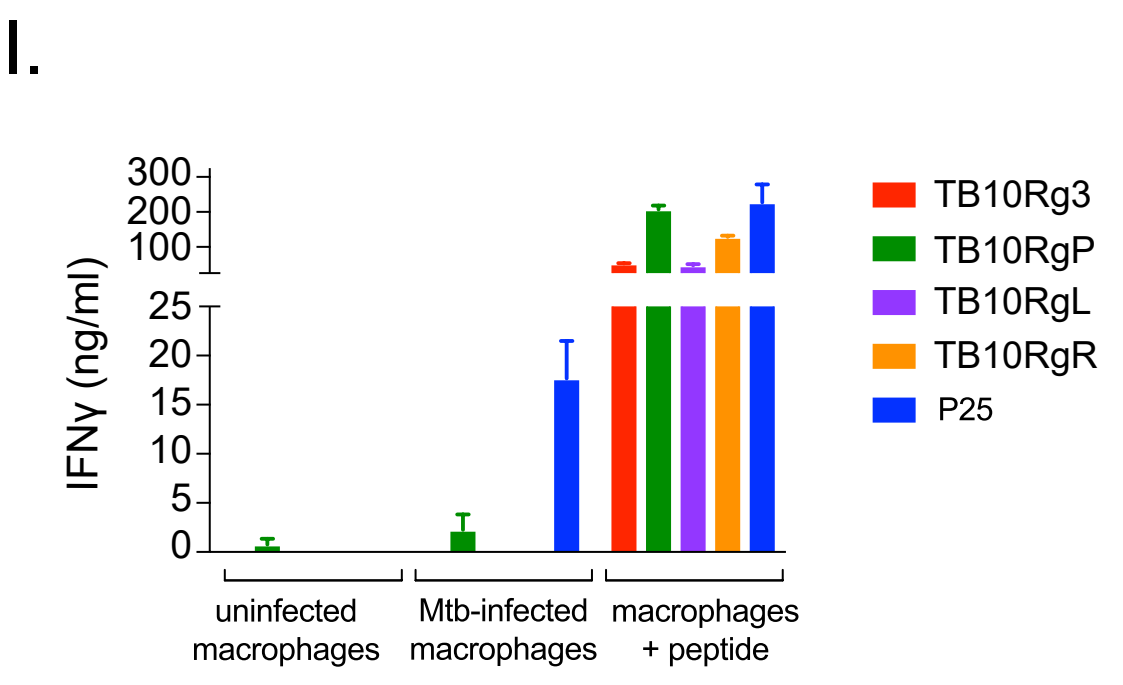
I.
IFNγ (ng/ml)
300
200
100
25
20
15
10
5
0
TB10Rg3
TB10RgP
TB10RgL
TB10RgR
P25
uninfected macrophages
Mtb-infected macrophages
macrophages + peptide

Figure 4.

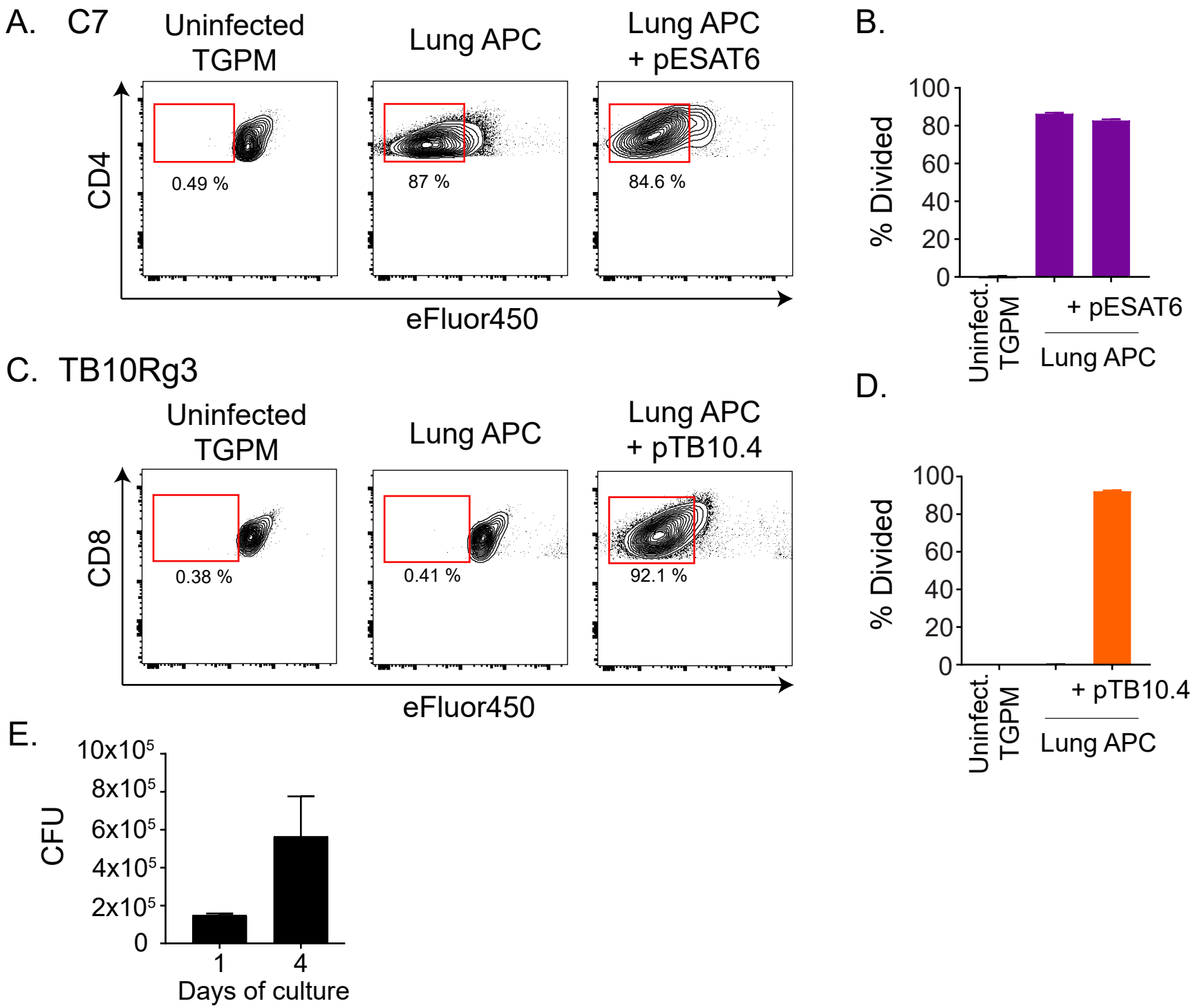
A. C7
Uninfected TGPM
Lung APC
Lung APC + pESAT6
CD4
0.49 %
87 %
84.6 %
eFluor450
B.
% Divided
100
80
60
40
20
0
Uninfect. TGPM
Lung APC
+ pESAT6
C. TB10Rg3
Uninfected TGPM
Lung APC
Lung APC + pTB10.4
CD8
0.38 %
0.41 %
92.1 %
eFluor450
D.
% Divided
100
80
60
40
20
0
Uninfect. TGPM
Lung APC
+ pTB10.4
E.
CFU
10x10^5
8x10^5
6x10^5
4x10^5
2x10^5
0
1
4
Days of culture

Figure 5.

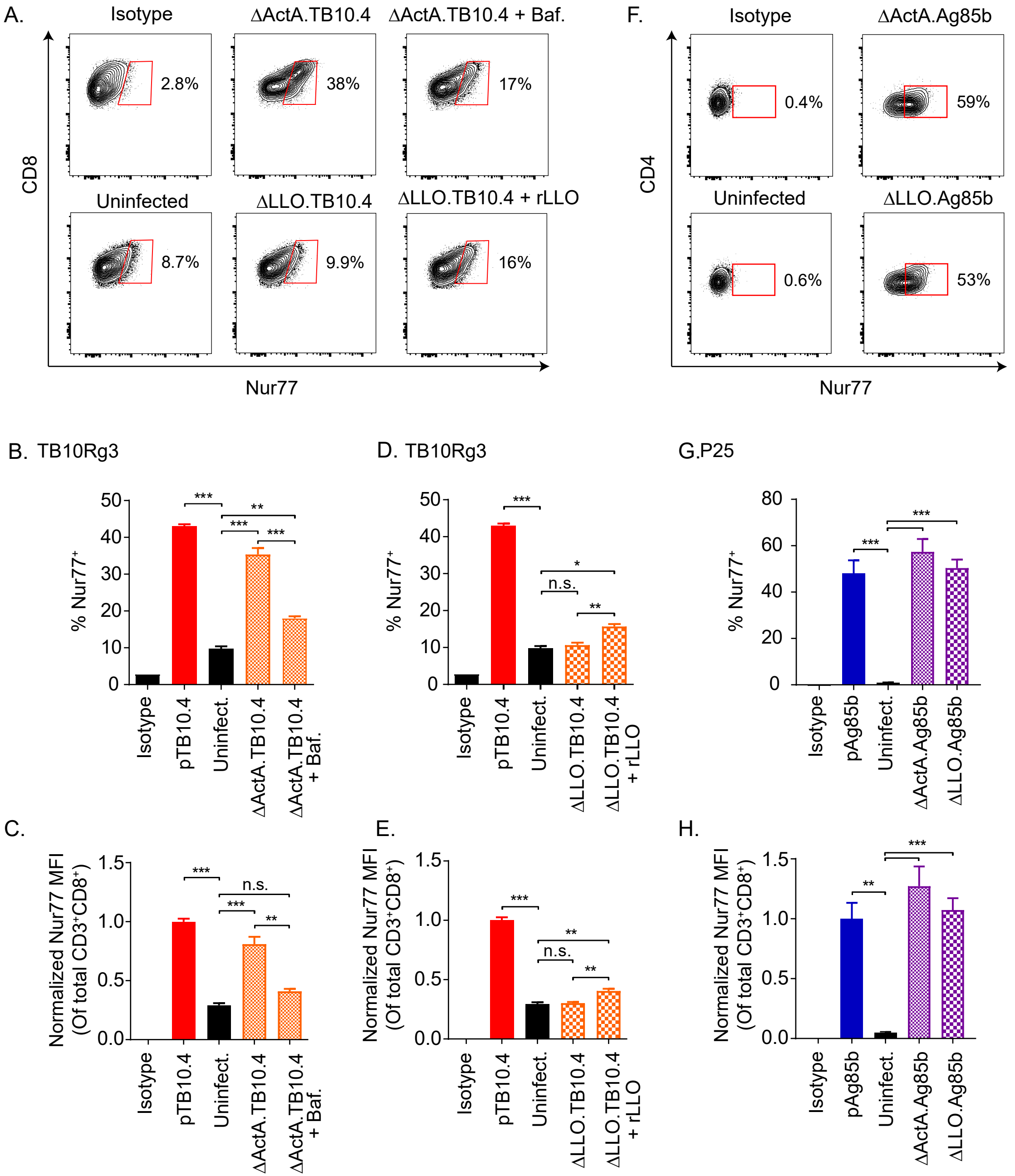
A.
Isotype
ΔActA.TB10.4
ΔActA.TB10.4 + Baf.
2.8%
38%
17%
Uninfected
ΔLLO.TB10.4
ΔLLO.TB10.4 + rLLO
8.7%
9.9%
16%
CD8
Nur77
F.
Isotype
ΔActA.Ag85b
0.4%
59%
Uninfected
ΔLLO.Ag85b
0.6%
53%
CD4
Nur77
B. TB10Rg3
% Nur77+
Isotype
pTB10.4
Uninfect.
ΔActA.TB10.4
ΔActA.TB10.4 + Baf.
D. TB10Rg3
% Nur77+
n.s.
Isotype
pTB10.4
Uninfect.
ΔLLO.TB10.4
ΔLLO.TB10.4 + rLLO
G.P25
% Nur77+
Isotype
pAg85b
Uninfect.
ΔActA.Ag85b
ΔLLO.Ag85b
C.
Normalized Nur77 MFI (Of total CD3+CD8+)
n.s.
Isotype
pTB10.4
Uninfect.
ΔActA.TB10.4
ΔActA.TB10.4 + Baf.
E.
Normalized Nur77 MFI (Of total CD3+CD8+)
n.s.
Isotype
pTB10.4
Uninfect.
ΔLLO.TB10.4
ΔLLO.TB10.4 + rLLO
H.
Normalized Nur77 MFI (Of total CD3+CD8+)
Isotype
pAg85b
Uninfect.
ΔActA.Ag85b
ΔLLO.Ag85b

Figure 6.

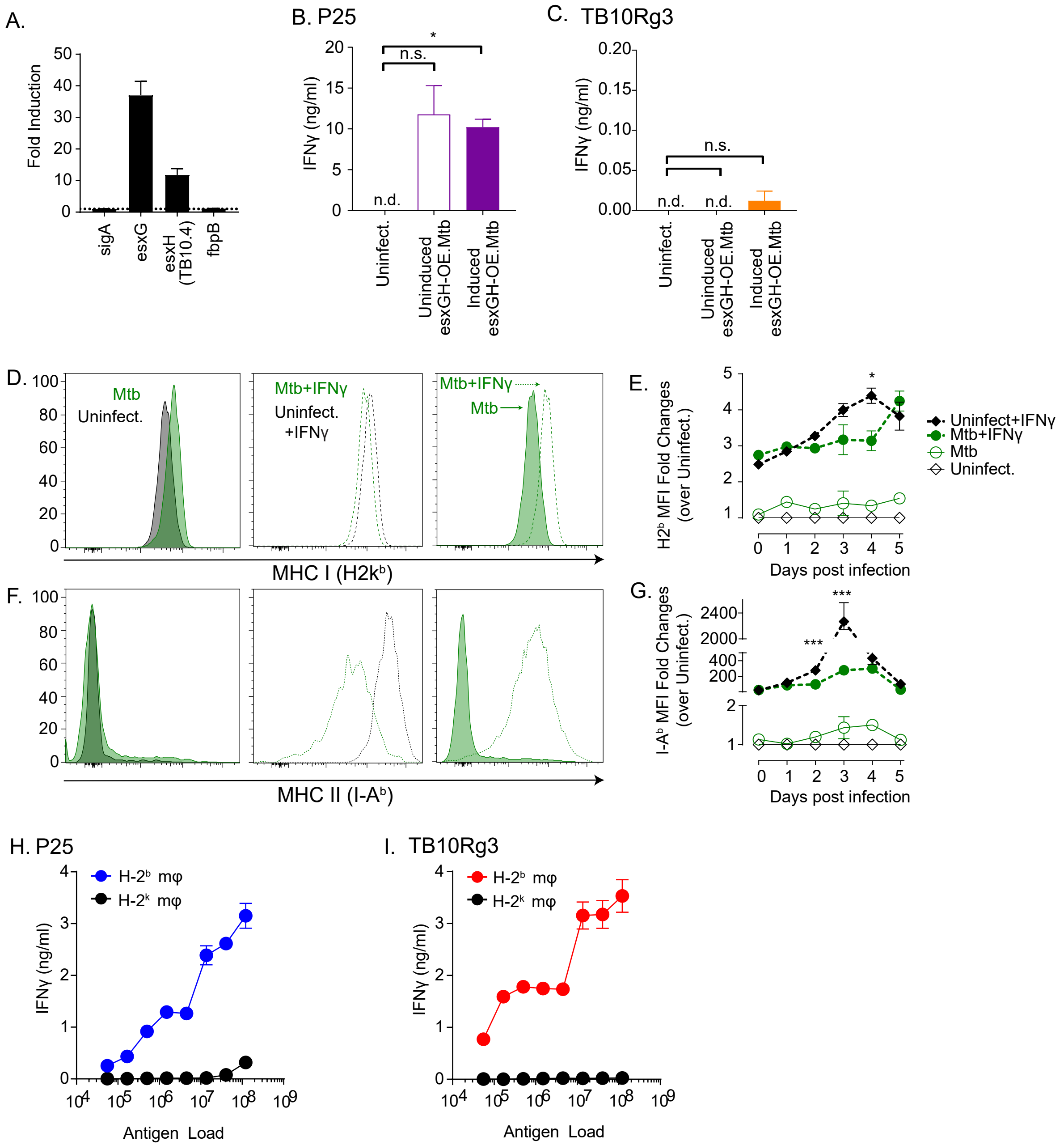
A.
Fold Induction
50
40
30
20
10
0
sigA
esxG
esxH (TB10.4)
fbpB
B. P25
IFNγ (ng/ml)
20
15
10
5
0
*
n.s.
n.d.
Uninfect.
Uninduced esxGH-OE.Mtb
Induced esxGH-OE.Mtb
C. TB10Rg3
IFNγ (ng/ml)
0.20
0.15
0.10
0.05
0.00
n.s.
n.d.
n.d.
Uninfect.
Uninduced esxGH-OE.Mtb
Induced esxGH-OE.Mtb
D.
Mtb
Uninfect.
Mtb+IFNγ
Uninfect. +IFNγ
Mtb+IFNγ
Mtb
MHC I (H2k^b)
E.
H2^b MFI Fold Changes (over Uninfect.)
*
Uninfect+IFNγ
Mtb+IFNγ
Mtb
Uninfect.
Days post infection
F.
MHC II (I-A^b)
G.
I-A^b MFI Fold Changes (over Uninfect.)
***
***
Days post infection
H. P25
H-2^b mφ
H-2^k mφ
IFNγ (ng/ml)
Antigen Load
I. TB10Rg3
H-2^b mφ
H-2^k mφ
IFNγ (ng/ml)
Antigen Load

Figure 7.

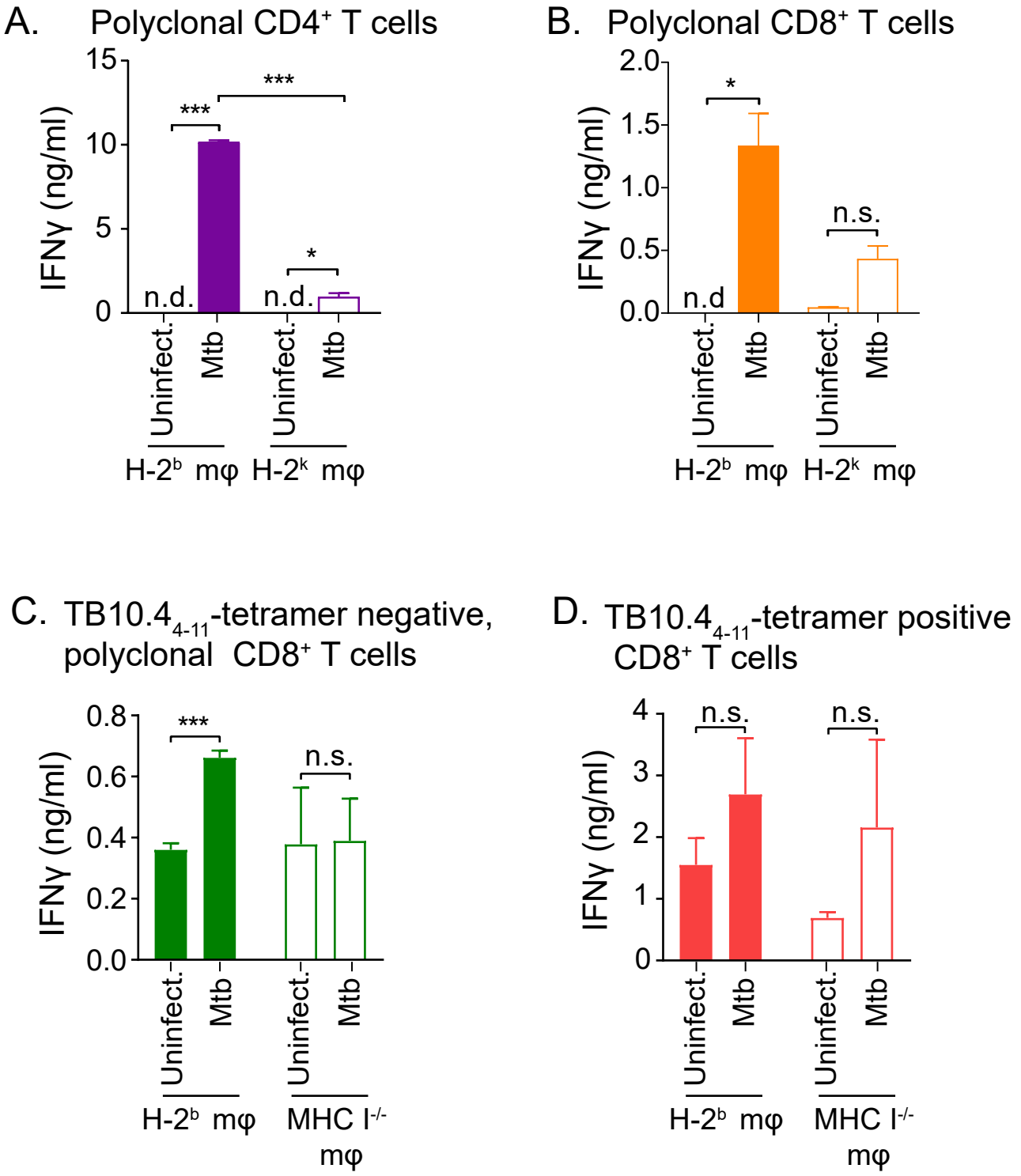
A. Polyclonal CD4+ T cells
IFNγ (ng/ml)
15
10
5
0
***
***
*
n.d.
n.d.
Uninfect.
Mtb
Uninfect.
Mtb
H-2b mφ
H-2k mφ
B. Polyclonal CD8+ T cells
IFNγ (ng/ml)
2.0
1.5
1.0
0.5
0.0
*
n.s.
n.d
Uninfect.
Mtb
Uninfect.
Mtb
H-2b mφ
H-2k mφ
C. TB10.4 4-11-tetramer negative, polyclonal CD8+ T cells
IFNγ (ng/ml)
0.8
0.6
0.4
0.2
0.0
***
n.s.
Uninfect.
Mtb
Uninfect.
Mtb
H-2b mφ
MHC I-/- mφ
D. TB10.4 4-11-tetramer positive CD8+ T cells
IFNγ (ng/ml)
4
3
2
1
0
n.s.
n.s.
Uninfect.
Mtb
Uninfect.
Mtb
H-2b mφ
MHC I-/- mφ

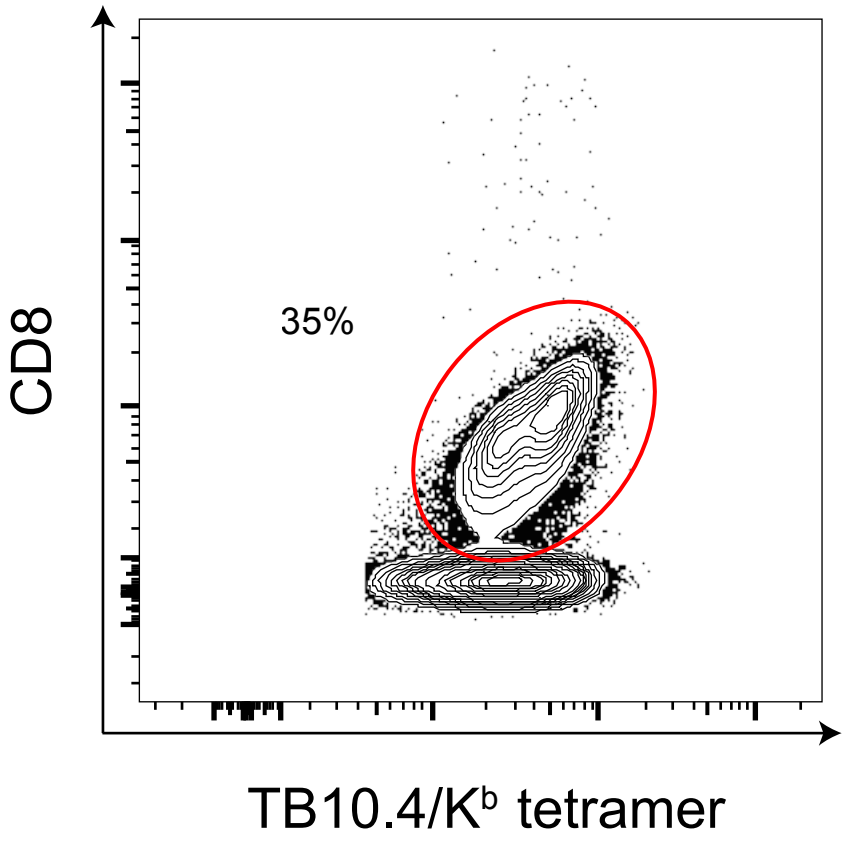

S1 Supplemental Figure

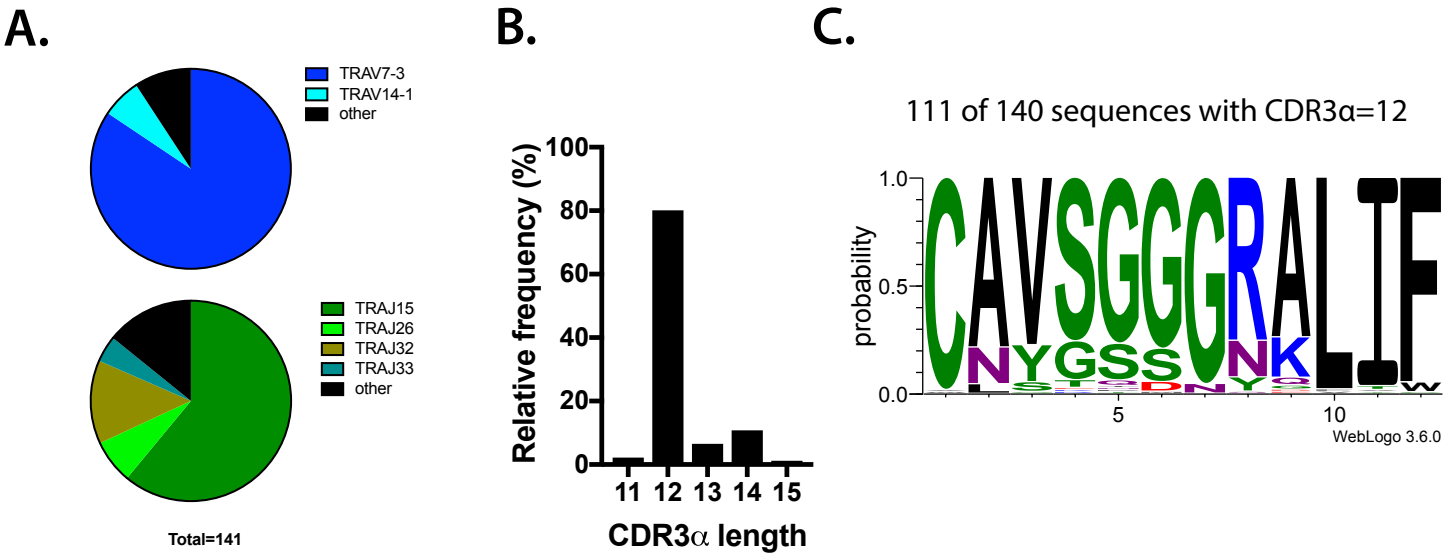

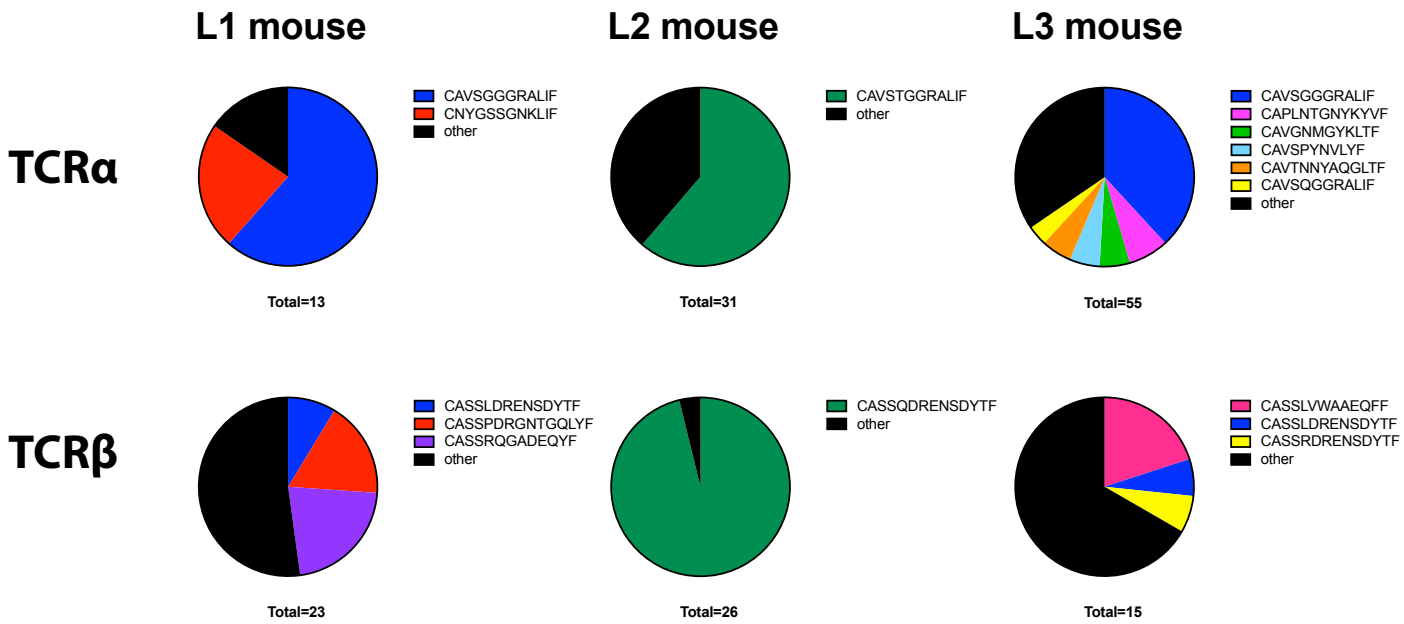

E.

	TCRα				TCRβ			
RgR	TRBV12-2	TRBD1	TRBJ2-2	CASSRDRENSDYTF	CAVSQGGRALIF	TRAV7-3	TRAJ15	L3
RgLD	TRBV12-2	TRBD1	TRBJ2-2	CASSLDRENSDYTF	CAVSGGGRALIF	TRAV7D-3	TRAJ15	L3
RgL	TRBV12-2	TRBD1	TRBJ2-2	CASSLDRENSDYTF	CAVSGGGRALIF	TRAV7-3	TRAJ15	L1
RgQ	TRBV2	TRBD1	TRBJ2-2	CASSQDRENSDYTF	CAVSTGGRALIF	TRAV7D-3	TRAJ15	L2
RgP	TRBV2	TRBD1	TRBJ2-2	CASSPDRGNTGQLYF	CNYGSSGNKLIF	TRAV7-3	TRAJ32	L1

S2 Supplemental Figure

A.

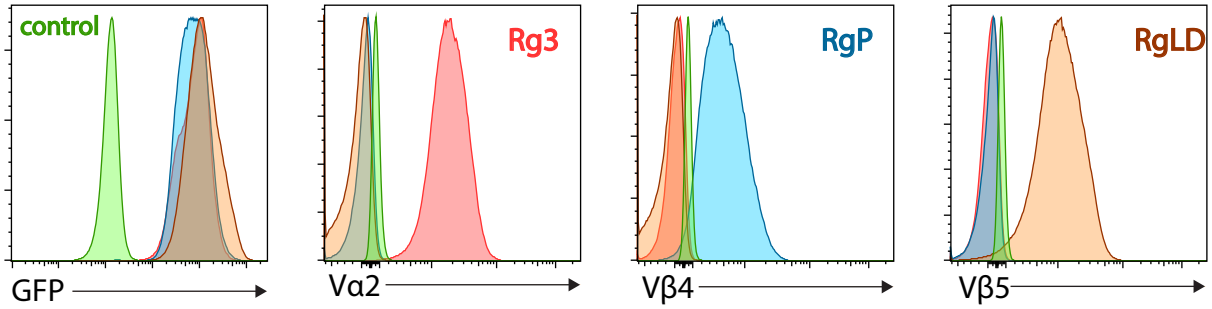

B.

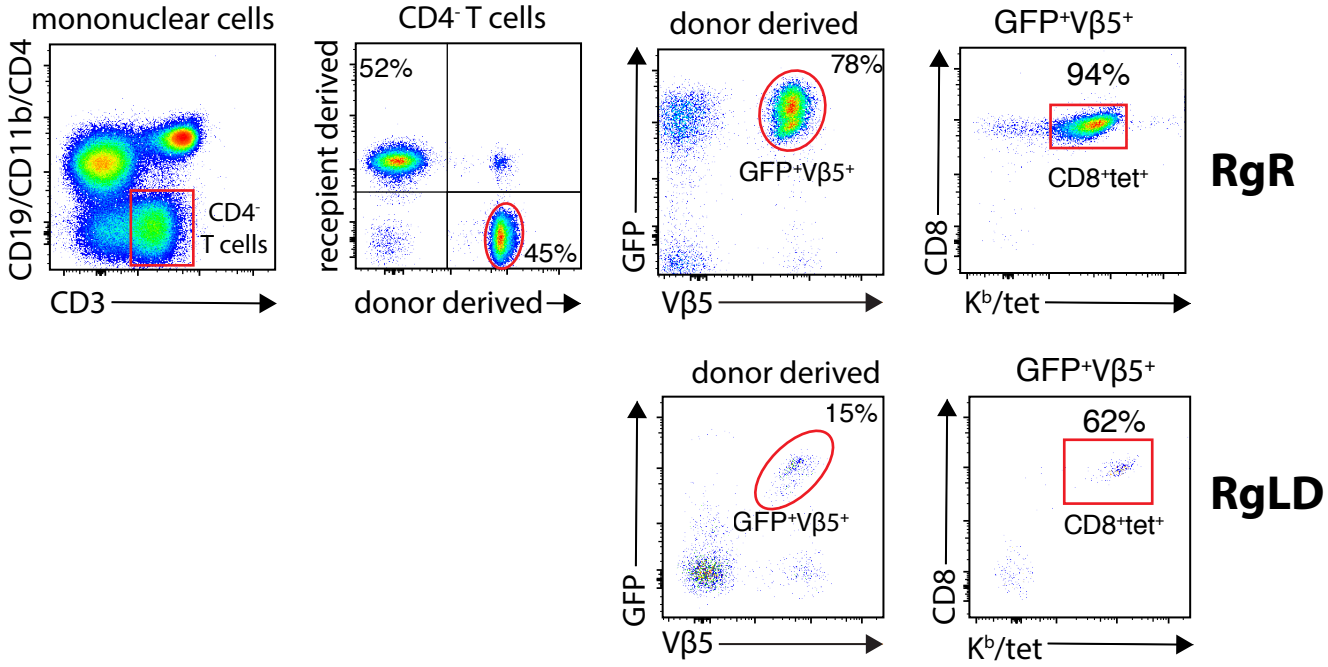

C.

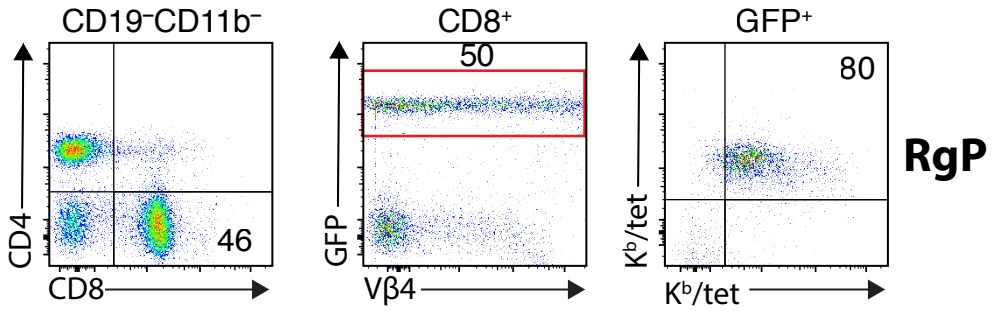

S3 Supplemental Figure